UNIVERSITY OF CALIFORNIA

Los Angeles

Faradaic Transistor for Investigating Electrochemical Interface

A dissertation submitted in partial satisfaction of the

requirements for the degree Doctor of Philosophy

in Materials Science and Engineering

by

Zhihong Huang

2021

ABSTRACT OF THE DISSERTATION

Faradaic Transistor for Investigating Electrochemical Interface

by

Zhihong Huang

Doctor of Philosophy in Materials Science and Engineering

University of California, Los Angeles, 2021

Professor Xiangfeng Duan, Co-Chair

Professor Yu Huang, Co-Chair

Electrocatalysis plays an essential role in various clean energy technologies, including fuel cells and electrolyzers. A fundamental understanding of the electrochemical processes on the electrode and electrolyte interface is of paramount importance for rational design of advanced catalysts. Direct monitoring the interface under operando condition is the most effective way to investigate interfacial reactions, however, the interface is buried between catalyst material and electrolyte and is thus notoriously difficult to probe.

Here in, I designed a faradaic transistor based on surface electron scattering effect, which provided surface specific information on the electrochemical interface. Reaction intermediates that adsorbed on catalyst surface can be directly monitored by detecting the conductance change of catalyst during a reaction. Faradaic transistor was firstly applied to investigate

hydrogen adsorption process on platinum nanowires (PtNWs) surface in electrochemical environment. The hydrogen adsorption in the entire potential range, including hydrogen underpotential deposition (H_{upd}) and hydrogen evolution reaction (HER) region, was successfully resolved. An overpotentially deposited hydrogen (H_{opd}) adsorption peak near equilibrium potential was observed for the first time. DFT calculation on nanowire with same surface structure revealed the H_{opd} is the hydrogen that adsorbed on the edge sites, which is considered as kinetically active reaction intermediate.

We later used faradaic transistor to investigate hydrogen adsorption behavior on PtNWs in solutions of different pH. A pH-dependent H_{opd} peak intensity was identified, which is correlated to the pH-dependent HER activity. DFT calculation also exhibited consistent results. Therefore, we proposed the HER reaction rate is governed by H_{opd} coverage. Further Tafel analysis demonstrated the reaction mechanism of HER is also determined by H_{opd} coverage. Combining theoretical and experimental results, we concluded that H_{opd} coverage is the unified descriptor for HER. Hydrogen adsorption on Pt/$Ni(OH)_2$ nanowire in alkaline solution was also investigated. Compared with pure PtNWs, much higher H_{opd} coverage was observed on Pt/$Ni(OH)_2$ surface in alkaline solution, which revealed the molecular-level origin of the improved HER activity on Pt/$Ni(OH)_2$ surface. Therefore, our findings not only offered new insight into understanding the relationship between adsorbed state of reaction intermediate and reaction kinetics, but also provide a governing principle for practical catalyst design.

The dissertation of Zhihong Huang is approved.

Yong Chen

Ximin He

Xiangfeng Duan, Committee Co-Chair

Yu Huang, Committee Co-Chair

University of California, Los Angeles

2021

Table of Contents

List of Figures

Acknowledgement

I am grateful for the opportunities to study and work at University of California, Los Angeles. My Ph. D journey will be one of the most important and memorable time in my life. I feel very lucky I can work in a group where the advisors are very talented and have great passion on scientific research and the students are energetic and helpful. I sincerely thank all the people who have inspired, encouraged, and enriched me.

Firstly, I want to thank my advisors, Professor Xiangfeng Duan and Professor Yu Huang for their continuous guidance and help during these years. In my first two years, I experienced a hard time when I started to do research in a newly emerging filed. They showed great patience on me and talked with me actively. They always showed great interest on the progress I made, which motivated and encouraged me a lot. Their keen insight gave me inspiration to explore the most critical issues in a research field. The way of thinking on scientific research is the most important thing I learnt from them, which will have a profound influence on my future academic career.

I would also like to thank my committee members, Professor Yong Chen and Professor Ximin He for their help in my qualification exam, oral defense exam and final dissertation. Their insightful comments and valuable advices help me to improve my research and myself.

I also want to thank my collaborators Dr. Tao Cheng, who is currently working in Soochow University, and Professor William Goddard from Caltech for their theory support. The discussion with them is always fruitful and helpful.

I also want to express my sincere appreciation to my group members. First of all, I would like to thank Dr. Mengning Ding, who is currently working in Nanjing University, for giving me

lots of help in early period of my research. His passion and curiosity on scientific research always inspired me. Secondly, I want to thank Guangyan Zhong, Chengzhang Wan, Peiqi Wang, Zhong Wan, Sibo Wang, Zipeng Zhao, Jin Cai, and Jin Huang and all other group members.

Biography

Zhihong Huang received his B.S. degree in Chemistry from University of Science and Technology of China in 2014. During his undergraduate, He worked in Professor Shuhong Yu's group. He then joined the Ph.D program in Materials Science and Engineering at University of California, Los Angeles in 2015. He conducted research under the guidance of Prof. Xiangfeng Duan and Prof. Yu Huang. His research focused on fundamental understanding of electrochemical processes on catalyst surface.

Chapter 1 Introduction

1.1 Electrocatalysis and electrode/electrolyte interface

Global warming is one of the most important issues in today's world. The consumption of nonrenewable fossil fuel is considered as the major cause. To mitigate this problem, one promising way is developing sustainable pathways to produce clean fuel. Hydrogen, as a carbon-free energy source, has attracted great attention. In order to effectively produce hydrogen, hydrogen evolution reaction (HER), which generated hydrogen by water splitting reaction, is considered as a sustainable way for hydrogen mass production. Compared with current industrial hydrogen production by steam reforming of natural gas, the electrochemical process is more environmentally friendly. The hydrogen can further be used as energy carrier in fuel cell, where hydrogen oxidation reaction (HOR) and oxygen reduction reaction (ORR) occur to generate electricity. Fuel cell is therefore considered as a promising clean energy supply for future automobile vehicle.

Electrocatalysis plays a central role in these clean energy technologies. To ensure the widespread application of these technologies, the main challenge is to develop affordable, durable and high-performance catalysts. Over the past several decades, substantial theoretical and experimental efforts have been made to understand the reaction mechanisms and governing principles of various electrochemical processes on catalyst surface, which provide rational guidance for practical catalyst design[1-2]. As with heterogeneous catalysis, the ultimate challenge in electrocatalysis is establishing the relationship between the reaction kinetics and adsorbed states of reaction intermediates[3]. In general, the adsorbed states of intermediate are strongly dependent on the properties of electrode and electrolyte interfaces (EEI), including the

intrinsic electronic properties of electrode materials and structure of electrical double layer (EDL).

The electronic properties of catalysts can be tuned by material engineering, which aims to increase the number of active sites on catalyst surface and improve the intrinsic activity of each site[1]. The structure of EDL is also vital for reaction kinetics. Many important processes, such as mass transportation, ion de-solvation, molecule adsorption/desorption and charge transfer, occur in the EDL during an electrochemical reaction.

The conventionally accepted model of EDL consist of two regions of ion distribution (see Fig. 1-1). The first layer, also called compact layer, consists of ions that strongly adsorbed on the surface. The second layer is diffuse layer, where ions are attracted to the surface by Coulomb force. In the compact layer, there are two types of adsorbed ions. Ions that directly adsorbed on the surface are called specifically adsorbed ions. Ions that at distance of their closest approach to the electrode are called non-specifically adsorbed ions[4]. The structure of double layer can affect the transport of reactant and product. For example, the structure of water network will affect proton and hydroxide transport through the double layer[5]. With reaction taking place on the electrode, the binding energy and coverage of reaction intermediates play a major role in governing the reaction kinetics[6-7]. Some spectator species that didn't participate in the reaction can also affect reaction rate. For example, the supporting anions in sulfuric acid electrolyte. The presence of spectator species reduces the number of available active sites and thus suppressed the reaction rate[8]. Therefore, reaction kinetics are governed by several parameters. In my work, I investigated the adsorption state of reaction intermediate, which is the major descriptor for reaction kinetics.

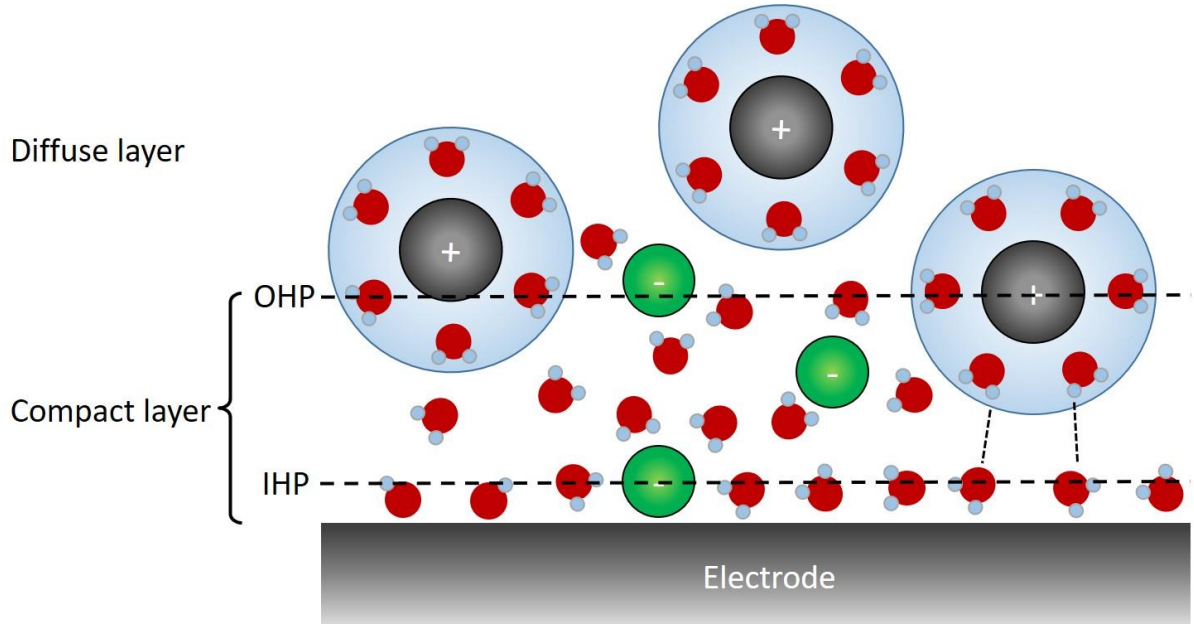

Figure 1-1 Schematic illustration of electrode/electrolyte interface. The inner Helmholtz plane (IHP) is the plane passes through the center of specifically adsorbed ions. The outer Helmholtz plane (OHP) is the plane passes through the center of non-specifically adsorbed ions in the compact layer.

1.2 Hydrogen evolution reaction and catalysis mechanism

HER is a model reaction of considerable significance for both fundamental electrochemistry and renewable fuel production. Due to the simplicity of HER, it is commonly used as a platform for investigating the relationship between reaction kinetics and adsorbed state of reaction intermediates. Many basic principles and concepts in electrochemistry are established by investigating HER, which built the foundation for understanding more complicated reactions. The reaction mechanism of HER is generally described by three elementary steps: Volmer step, Heyrovsky step, and Tafel step. In acidic solution, hydronium is the hydrogen donor, reaction mechanism is showed as follows.

$$H_3O^+ + e^- + M \rightarrow M - H + H_2O \quad \text{(Volmer step)} \tag{1.1}$$

$$H_3O^+ + e^- + M - H \rightarrow M + H_2 + H_2O \quad \text{(Heyrovsky step)} \tag{1.2}$$

$$2M - H \rightarrow 2M + H_2 \quad \text{(Tafel step)} \tag{1.3}$$

In base solution, water is the hydrogen donor, the reaction mechanism is showed as follows.

$$H_2O + e^- + M \rightarrow M - H + OH^- \quad \text{(Volmer step)} \tag{1.4}$$

$$H_2O + e^- + M - H \rightarrow M + H_2 + OH^- \quad \text{(Heyrovsky step)} \tag{1.5}$$

$$2M - H \rightarrow 2M + H_2 \quad \text{(Tafel step)} \tag{1.6}$$

In these elementary steps, adsorbed hydrogen (H_{ad}) is the sole reaction intermediate. Conventional mechanistic studies have correlated the HER reaction rate with hydrogen binding energy following Sabatier principle[7]. Platinum (Pt) has optimal interaction with hydrogen intermediate and thus has been demonstrated as the most efficient catalyst for HER. However, it has long been known that the HER reaction rate on Pt in base solution is two orders of magnitude slower than that in acidic solution. Molecular-level understanding of the origin of this problem is essential for development of alkaline electrolyzers. In my work, I examined the adsorption behavior of hydrogen intermediates and provided a new insight into the origin of this pH-dependent HER activity.

1.3 Surface electron scattering effect

To monitor molecule or atom adsorption behavior on Pt surface, a physical or chemical parameter that is surface-sensitive is needed. It has long been known in surface science that the conductivity of metallic material can be affected by its surface condition. This phenomenon is mostly described by the surface electron scattering theory of Fuchs and Sondheimer[9]. According to their theory, part of electrons will be diffusively scattered at the surface and suffer a significant momentum change, leading to the conductivity decrease. The conductivity of

metallic nanowires can be described by two formulas[9].

$$\frac{\sigma_0}{\sigma} = 1 + \frac{3}{4}(1-p)\frac{l}{d} \quad (d \gg l) \tag{1.7}$$

$$\frac{\sigma_0}{\sigma} = \frac{(1-p)}{(1+p)}\frac{l}{d} \quad (d \ll l) \tag{1.8}$$

Where σ_0 is the conductivity of bulk material, σ is the conductivity of nanowire, l is mean free path of electrons in bulk material, d is the diameter of nanowire, p, also called specularity parameter, is the fraction of electrons that are specularly reflected on the surface without any losses of momentum component in its direction. Foreign atoms that adsorbed on the surface can increase the diffusive scattering of conduction electrons, which reduces p and therefore makes conductivity decrease. For bulk materials, this conductance change is negligibly small, so that it is practically impossible to detect it. However, when the size of the material is comparable to the mean free path of electron, its conductivity can be strongly affected by surface conditions. Additional evidence also indicated the specularity change is proportional to the coverage of adsorbates[10]. Based on this principle, conductance measurement has been demonstrated as an effective way for probing ionic and molecular adsorption on electrochemical interface[11-13]. However, up to now, most researches were conducted on metallic thin films or nanowires, where the surface is ill-defined and multiple surface sites exist on the surface. And most electrochemical processes studied is in mild condition. In my work, ultrathin Pt nanowires with well-defined surface structure is employed to study hydrogen adsorption process at potential where hydrogen generation with large faradaic current is occurring on the surface. The high sensitivity of the nanowire ensured the identification of hydrogen adsorption on different sites.

1.4 References

1. Seh, Z. W.; Kibsgaard, J.; Dickens, C. F.; Chorkendorff, I.; Nørskov, J. K.; Jaramillo, T. F., Combining theory and experiment in electrocatalysis: Insights into materials design. *Science* **2017,** *355* (6321), eaad4998.

2. Stamenkovic, V. R.; Strmcnik, D.; Lopes, P. P.; Markovic, N. M., Energy and fuels from electrochemical interfaces. *Nature Materials* **2016,** *16*, 57.

3. Zheng, Y.; Jiao, Y.; Vasileff, A.; Qiao, S.-Z., The Hydrogen Evolution Reaction in Alkaline Solution: From Theory, Single Crystal Models, to Practical Electrocatalysts. *Angewandte Chemie International Edition* **2018,** *57* (26), 7568-7579.

4. Zhang, L. L.; Zhao, X. S., Carbon-based materials as supercapacitor electrodes. *Chemical Society Reviews* **2009,** *38* (9), 2520-2531.

5. Ledezma-Yanez, I.; Wallace, W. D. Z.; Sebastián-Pascual, P.; Climent, V.; Feliu, J. M.; Koper, M. T. M., Interfacial water reorganization as a pH-dependent descriptor of the hydrogen evolution rate on platinum electrodes. *Nature Energy* **2017,** *2*, 17031.

6. Conway, B. E.; Tilak, B. V., Interfacial processes involving electrocatalytic evolution and oxidation of H2, and the role of chemisorbed H. *Electrochimica Acta* **2002,** *47* (22), 3571-3594.

7. Skúlason, E.; Tripkovic, V.; Björketun, M. E.; Gudmundsdóttir, S.; Karlberg, G.; Rossmeisl, J.; Bligaard, T.; Jónsson, H.; Nørskov, J. K., Modeling the Electrochemical Hydrogen Oxidation and Evolution Reactions on the Basis of Density Functional Theory Calculations. *The Journal of Physical Chemistry C* **2010,** *114* (42), 18182-18197.

8. Strmcnik, D.; Lopes, P. P.; Genorio, B.; Stamenkovic, V. R.; Markovic, N. M., Design principles for hydrogen evolution reaction catalyst materials. *Nano Energy* **2016,** *29*, 29-36.

9. Sondheimer, E. H., The mean free path of electrons in metals. *Advances in Physics* **2001,** *50* (6), 499-537.

10. Wißmann, P., The electrical resistivity of pure and gas covered metal films. In *Surface Physics*, Springer Berlin Heidelberg: Berlin, Heidelberg, 1975; pp 1-96.

11. Rath, D. L., Studies of electrode resistance in the electrochemical cell. *Journal of Electroanalytical Chemistry and Interfacial Electrochemistry* **1983,** *150* (1), 521-534.

12. Fujihara, M.; Kuwana, T., Studies of electrochemical interfaces of thin PT film electrodes by surface conductance. *Electrochimica Acta* **1975,** *20* (8), 565-573.

13. Ding, M.; He, Q.; Wang, G.; Cheng, H.-C.; Huang, Y.; Duan, X., An on-chip electrical transport spectroscopy approach for in situ monitoring electrochemical interfaces. *Nature Communications* **2015,** *6*, 7867.

Chapter 2 Faradaic transistor for probing reaction intermediates of hydrogen evolution reaction on platinum surface

2.1 Introduction

Successful deployment of hydrogen-based energy technologies relies strongly on our understanding of the electrochemical processes occurring on the electrode/electrolyte interface. This electrochemical interface consists of catalyst surface and electrical double layer (EDL). Its physical and chemical properties directly determine the chemistry of the electrochemical processes happening on the surface. For surface scientist and electrochemists, the ultimate objective is to elucidate the relationship between reaction kinetics and the properties of electrochemical interface. Continued theoretical and experimental works over recent decades have established a framework to understand the catalytic trends on a series of catalysts[1-4]. However, the structure of EDL is rarely discussed because this layer is only several or tens of nanometers thick, which located between catalyst surface and electrolyte. It is difficult to be accessed by conventional spectroscopy approaches.

Several techniques have been attempted to study EDL. X-ray Spectroscopy (XAS) has been demonstrated to be an effective tool for examining the surface properties of materials due to the intrinsic shallow penetration depth of electrons and soft X-ray photons, which provides element-specific information near the surface region[5-6]. Vibration spectroscopies, such as infrared absorption (IR) and Raman spectroscopy, have also been used to characterize reaction intermediates on catalyst surface[7-9]. However, in terms of quantitatively or semi-quantitatively estimating the coverage of reaction intermediates on catalyst surface, it is difficult to be realized by conventional spectroscopy techniques. In the mechanistic study of electrochemical reactions

on surface, the coverage of reaction intermediates is of major interest[10]. Therefore, a technique that can detect reaction intermediates in electrochemical environment and integrally measure its coverage is of considerable significance for in-depth understanding of the reaction mechanism and reaction kinetics.

It has long been known that the conductivity of ultrathin nanostructure can be affected by processes occurring on its surface. Fuchs and Sondheimer firstly attributed this conductivity change to the altered electron scattering on the surface[11]. According to their theory, the conduction electrons is partially diffusively scattered on the surface. Molecule that adsorbed on the surface can induce formation of new scattering centers on the surface and increase diffusive scattering, leading to decrease of conductivity. This principle has been used to study gas adsorption for many years[12-14]. And it is later extended to examine more complicated electrochemical interface, where ionic and molecular adsorption is precisely controlled by potential applied on the electrode[15-18]. Since conductance measurement is an integral measurement that takes account of scattering effect of each surface site, the conductance change is directly correlated to coverage of surface adsorbates. However, previous studies were mostly conducted on metal thin film with ill-defined surface structure, which made it difficult to resolve adsorption of reaction intermediates on different surfaces and different sites and thus hindered the kinetics analysis of electrochemical reactions.

Here, we designed a nanodevice that used ultrathin platinum nanowires (PtNWs) with well-defined surface structure as catalyst to detect hydrogen adsorption in an electrochemical environment. Two independent channels were applied to concurrently monitor the electrochemical current and conductance change of PtNWs at different potential. The

underlying principle is analogous to conventional field effect transistor, where an electrostatic field is applied to modulate the conductance of the channel. Here, in our system, the conductance of the PtNWs is modulated by interfacial faradaic process. Therefore, we designated this nanodevice as a faradaic transistor.

Since only hydrogen adsorption and accompanied water desorption are responsible for conductance change in the interested potential range (0.40 to -0.10V vs. RHE), a highly specific conductance change associated with hydrogen adsorption can be monitored in real time with the sweeping of electrochemical potential. By differentiating the conductance change, the derivative conductance change showed close resemblance to voltametric current. Importantly, since the conductance is only sensitive to surface adsorbed hydrogen (H_{ad}) and won't be affected by large faradaic current and H_2 produced, this approach allows directly monitoring of both underpotentially deposited hydrogen (H_{upd}) and overpotentially deposited hydrogen (H_{opd}) in HER region, which cannot be realized by conventional cyclic voltammetry (CV) approach. In this way, we, for the first time, discovered a H_{opd} adsorption peak that appeared at the onset of HER. DFT calculation on nanowire with same surface structure showed that this H_{opd} peak originated from hydrogen adsorbed on the edge sites. It also proved this H_{opd} is the kinetically active reaction intermediate of HER.

2.2 Device preparation and characterization

Synthesis of Pt/NiO nanowires

Pt/NiO nanowires were prepared following previous methods[19]. In a typical synthesis, 20mg $Pt(acac)_2$, 30mg $Ni(acac)_2$,1.6mg $W(CO)_6$, 60mg PVP (mw. 40,000) and 135mg glucose were dissolved in mixture of 2mL 1-octadecene (ODE) and 3mL oleylamine (OAm). After sonicated for 15 min, the mixture was sealed with nitrogen. Then the mixture was heated up to 140℃

and kept for 4 hours. After cooling down to room temperature, the as-synthesized nanowires were washed with cyclohexane/ethanol mixture for several times and then dispersed in 5mL ethanol for use.

Preparation of device

A SiO2/Si substrate pre-deposited with gold electrodes was firstly covered with a layer of PMMA (A8, MicroChem Corp.) by spin coating. Then E-beam lithography was applied to open windows on paired electrodes to form a template. After that, the Pt/NiO nanowires suspension was dropped slowly into a beaker filled with water. A black film of Pt/NiO was then formed on the water surface. Then, Pt/NiO nanowires film was transferred onto the substrate by an immerge-and-lift process. The PMMA template layer was later dissolved in acetone and the film deposited in the opened window is still remained on the substrate. The NiO on the PtNWs was then dissolved by immerging the device in 0.1M perchloric acid solution for 1min. A layer of PMMA then covered on the device again and the device was baked at 90℃ for 2h. Then, a window between the gold electrodes was opened to expose the nanowires for measurement. Before electrochemical measurements, the nanowires were activated by CV cycling in 0.1M $HClO_4$ for 150 cycles. The schematic illustration of device preparation is shown in Fig 2-1.

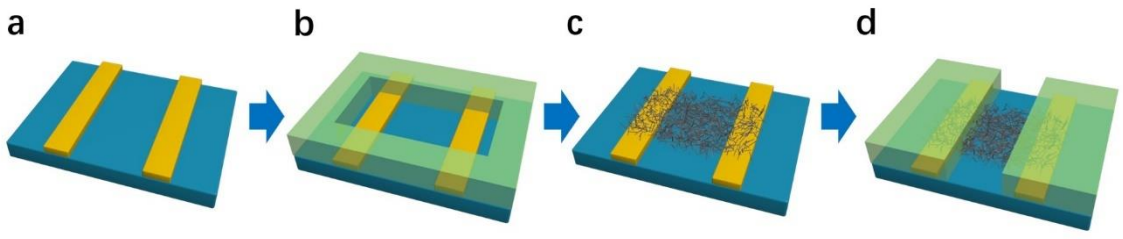

Figure 2-1 Schematic illustration of device fabrication. (a) SiO_2/Si substrate with pre-deposited gold electrodes. (b) The substrate was covered with a PMMA layer, and a window was opened on gold electrodes to form a template. (c) A Pt/NiO nanowires film was transferred

onto the template and PMMA was then dissolved. (d) After acid treatment, a PMMA layer was coated on device, and a window was then opened to expose nanowires.

Characterizations

Transmission electron microscopy (TEM) study showed that the as-synthesized Pt/NiO nanowires exhibited a core/shell structure with a higher contrast Pt core and lower contrast NiO shell. The nanowires have a diameter of 5-7 nm and a length of about 200-300 nm (see Fig. 2-2a,b). The TEM image of nanowires after 150 cycles of CV cycling showed the NiO shell has dissolved during electrochemical activation and a PtNW core of diameter of 2 nm remained (see Fig. 2-2c). The morphology of as-prepared device is also examined by scanning electron microscopy (SEM), as shown in Fig. 2-2d.

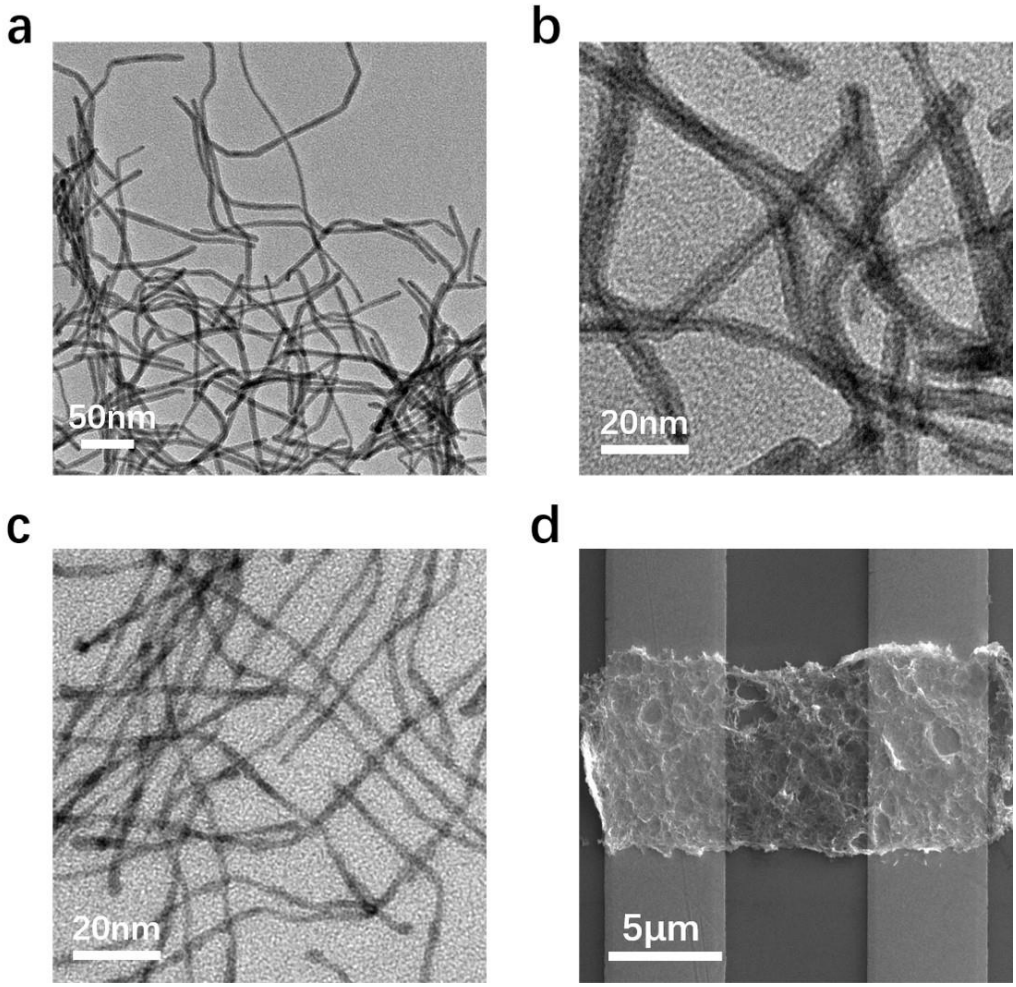

Figure 2-2 Morphology of Pt/NiO nanowires, PtNWs, and device. (a,b) TEM images of Pt/NiO core/shell nanowires. (c) TEM image of PtNWs after electrochemical activation. (d) SEM image of as-prepared device after acid treatment.

2.3 Results and discussion

Two independent channels are used in our experimental setup (see Fig. 2-3a). One channel is between drain and source (the gold electrodes). A lock-in amplifier was used to apply an alternating current (AC) signal between source and drain, which allows the in-situ measurement of conductance of PtNWs. Another channel is three electrodes system, which consists of a working electrode (PtNWs), a counter electrode (Pt wire), and a reference electrode (Ag/AgCl reference). The potential of PtNWs was modulated by a standard source measure unit (SMU), and a direct current (DC) signal can be recorded. This channel allows the measurement of CV current. Since these two channels have different types of current, they are independent and can be completely decoupled from each other. To ensure the efficient transport of reaction reactants and products on the catalyst surface, a microfluid system is set up for electrolyte refreshing (Fig. 2-3b). The microfluid system allows fresh electrolytes to fast flow over the working electrode. By controlling the flow rate, the diffusion of reactants and products on Pt surface can be greatly improved, which allows study of reaction of large faradaic current, such as HER.

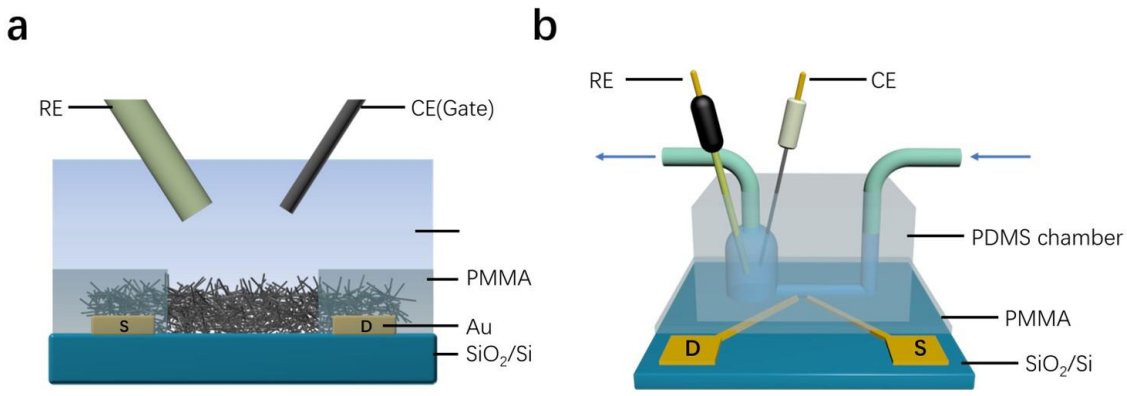

Figure 2-3 Schematic illustration of experimental setup. (a) Schematic illustration of two independent channels for in-situ CV and conductance measurement. (b) Schematic illustration of microfluid system for electrolyte refreshing. Blue arrows show the flow direction of electrolyte.

A typical profile of on-chip CV and conductance change measured in 0.1M perchloric acid solution is showed in Fig. 2-4a. The on-chip CV exhibited common features of Pt electrodes. Two different regions can be identified on the CV profile: 0.05-0.40V, where adsorption of H_{upd} occurs; and 0.40-0.70 V, which is the so-called double layer (D.L.) region. It is found the conductance change of PtNWs also experienced two different regions with different increasing rates.

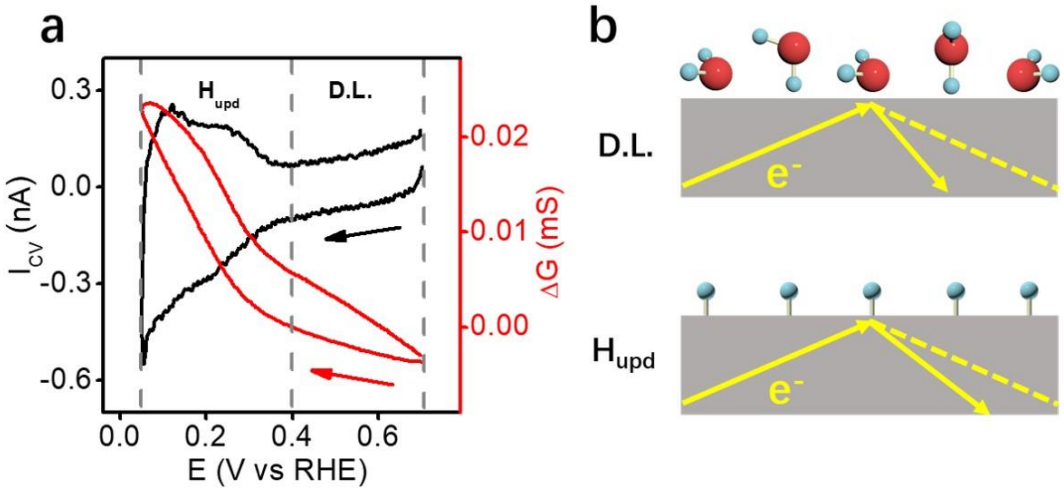

Figure 2-4 In-situ CV and conductance change of PtNWs. (a) In-situ CV (black curve) and concurrent conductance change (red curve) of PtNWs in N_2-saturated 0.1M $HClO_4$. The scan rate is 50mV s^{-1}. Here, 0.4V, the onset potential of hydrogen adsorption, is defined as the potential where conductance change is zero. (b) Schematic illustration of electron momentum change during scattering at the water-covered surface and hydrogen covered surface.

In the double layer region, The Pt surface is predominantly covered by a layer of water. The conductance slightly increased with decreasing the potential due to the field effect. Different with the surface molecular adsorption effect, field effect is conductance change with surface charge density induced by the applied electrical field. It is considered to have a significant contribution to conductance when the size of materials is comparable to the mean free path of electrons[20]. The relative conductance change due to field effect can be expressed as[15]:

$$\frac{\partial \sigma}{\sigma} = \alpha \frac{\partial N}{N} = \alpha \frac{\partial q}{q} \tag{2.1}$$

Where N is total number of conduction electrons, q is total free electronic charge. α is a proportionality constant. Therefore, introducing negative charges or withdrawing positive

charges on metallic nanomaterials will linearly increase the conductance, which is proportional to the number of charges added or removed. Such linearity has also been observed on thin gold film and porous nanocrystalline Pt in the double layer region[21-22]. Since lowering the potential of PtNWs was accompanied by removal of positive charges or accumulation of negative charge on the surface, the conductance of PtNWs gradually increase during this process.

A substantial conductance increase was observed in the H_{upd} region due to the adsorption of hydrogen. However, this seemingly contradicted the surface scattering theory, that predicted adsorption of molecule on clean surface would lead to conductance decease. Therefore, our results indicated hydrogen atom didn't adsorb on "bare" surface sites but on surface sites that are pre-occupied by water molecules, so the conductance change in H_{upd} region should take account of the scattering effect of both hydrogen atom and water. The apparent conductance increased with adsorption of hydrogen, which suggests water molecules have stronger scattering effect than hydrogen atom. The schematic of scattering process on water-covered and hydrogen-covered surface were illustrated in Fig. 2-4b.

The generally accepted step of hydrogen adsorption (or Volmer step) is hydrogen adsorb on unoccupied surface sites, as shown in eq.1.1, whereas our results indicated the Volmer step is a replacement reaction (eq. 2.2).

$$H_3O^+ + e^- + M - H_2O \rightarrow M - H + 2H_2O \quad (2.2)$$

This is in agreement with the apparent hydrogen binding energy (HBE_{app}) theory proposed by Zheng et al. that the H_{upd} peak position is determined by intrinsic hydrogen binding energy (HBE) and the water adsorption energy[23]. This hypothesis was verified by Cheng et al[24]. They carried out quantum mechanics molecular dynamics simulation to simulate water/Pt(100)

interface in H_{upd} region and found the water adsorption energy is the major cause for shift of H_{upd} peak position, which is related to HER activity. Therefore, our experiment provided direct evidence that adsorption of hydrogen is accompanied with desorption of water, which is of considerable significance for understanding HER activity from perspective of water adsorption behavior.

Since conductance is an integral measurement that takes account of scattering effect of each surface sites. the conductance change in H_{upd} region is directly correlated to hydrogen coverage. On the other hand, derivative of conductance change is expected to be correlated to hydrogen adsorption current at each potential. As shown in Fig. 2-5a, the derivative conductance change exhibited close resemblance to the CV curve in hydrogen adsorption branch. Especially, the peak appeared at 0.2V, which is commonly considered as hydrogen adsorption on Pt(100) facet[25], was also resolved in derivative result. Field effect has minority contribution to the conductance change in the H_{upd} region. Due to the linear relationship between field effect induced conductance change and potential, the derivative of this part of conductance change should be a constant, which does not affect profile of the overall derivative conductance change. By plotting the derivative conductance change as a function of voltametric current in H_{upd} region (Fig. 2-5b), a linear region was observed at potential of 0.17-0.5V, which validated the concept of linearity between conductance and coverage of adsorbates[12]. However, at potential close to the equilibrium potential, a significant deviation between CV current and derivative conductance change was observed. This is because, at potential near equilibrium potential, minority HER current also contributes to the CV current. To validate this assumption, the charge consumed/generated during hydrogen adsorption/desorption processes were calculated.

As shown in Fig. 2-5c, the charge consumed during hydrogen adsorption process was much larger than that generated in desorption process. Since the solution is N_2-saturated, during hydrogen desorption process, the charge only originated from oxidation of adsorbed hydrogen. However, in hydrogen adsorption process, protons can infinitely supply to the surface, which make it possible to locally generate small amount of H_2, especially at potential near equilibrium potential. Therefore, different from CV approach that records the overall charge transferred on surface, the conductance measurement simply resolved the associated adsorption process, which give faradaic transistor some unique advantages over CV approach. Specifically, for the surface processes that have no charge transfer, reactions with multiple charge transfer steps, or reactions that have large faradaic current involved, CV cannot provide information about the adsorption process on surface, while faradaic transistor can specifically monitor the adsorption process, which provides insight into in-depth understanding of reaction mechanisms and reaction kinetics.

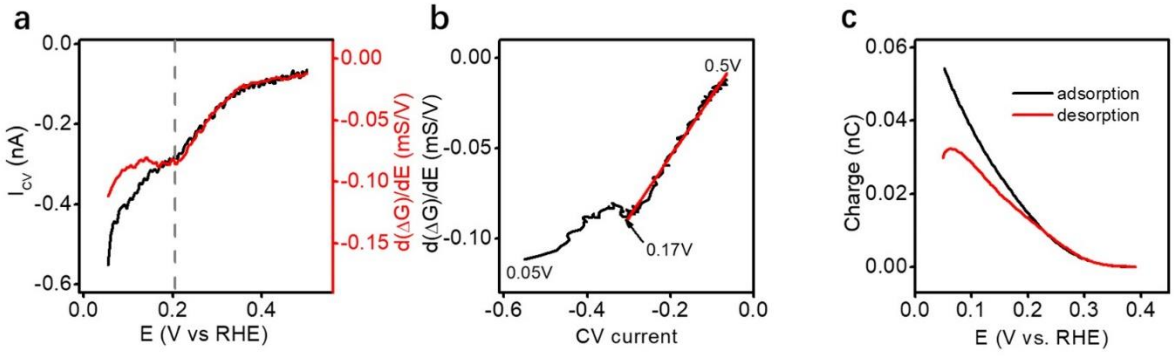

Figure 2-5 (a) Derivative conductance change and CV current in hydrogen adsorption branch. (b) Derivative conductance change as a function of CV current at each potential. Red line is linear fitting of results at potential from 0.50V to 0.17V (c) Charge consumed/generated in hydrogen adsorption/desorption process. Results were calculated based on on-chip CV.

The conductance measurement was then extended to the HER region, where a large faradaic current generated on surface. As shown in Fig. 2-6a, the CV current in the HER region is much larger than the H_{upd} current in Fig. 2-4a, so that the current response for hydrogen adsorption in the HER region is completely masked by HER current and thus cannot be directly detected by CV approach. However, the conductance of PtNWs kept increasing till potential of -0.1V, which suggested additional hydrogen adsorbed in HER region. By differentiating the conductance change and comparing it with the CV curve, two hydrogen adsorption peaks were resolved (see Fig. 2-6b). Besides the commonly observed H_{upd} peak at 0.2V, a new hydrogen adsorption peak appeared at 38mV, which is also overlapped with the onset potential of HER. Considering the hydrogen adsorbed at potential higher than 0.05V is normally assigned as H_{upd}, we assign this peak at lower potential as H_{opd}.

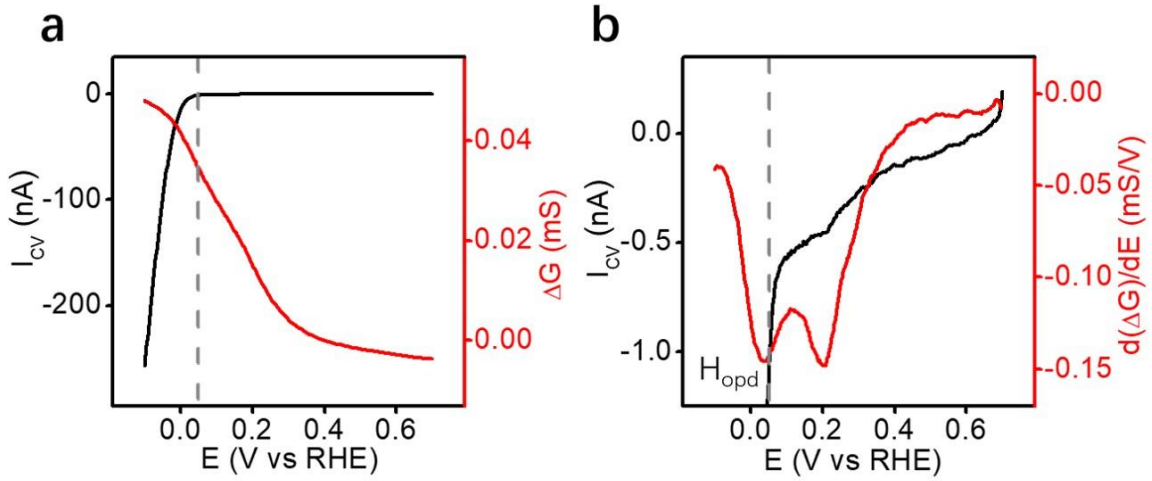

Figure 2-6 (a) In-situ CV and conductance change of PtNWs in potential range of (-0.1-0.7V). Dashed line is at potential of 0.05V (b) Comparison of derivative conductance change and CV profiles.

To further understand the adsorption sites of H_{opd}, we examined the surface structure of

activated PtNWs and carried out DFT calculation to simulate hydrogen adsorption behavior on nanowire of same surface structure. High-resolution TEM (HRTEM) images were recorded on the cross-section of activated PtNWs to identify the dominant facets on the surface. As shown in Fig. 2-7a, a hexagonal cross-section with well-defined facets was observed on most nanowires. The lattice-resolved image showed lattice fringes with spacing of 0.23nm and 0.19nm, corresponding to the (111) and (200) lattice planes of Pt, respectively (Fig. 2-7b). Therefore, it is found the surface of nanowire consists of 4(111) and 2(100) facets, which is consistent with the equilibrium shape predicted by Wulff construction[26-27]. Further analysis of growth direction of nanowires showed the nanowires grow along <110> direction (Fig. 2-7c), which yielded a surface with lowest energy, including 4(111) and 2(100). The schematic of surface structure is illustrated in Fig. 2-7d.

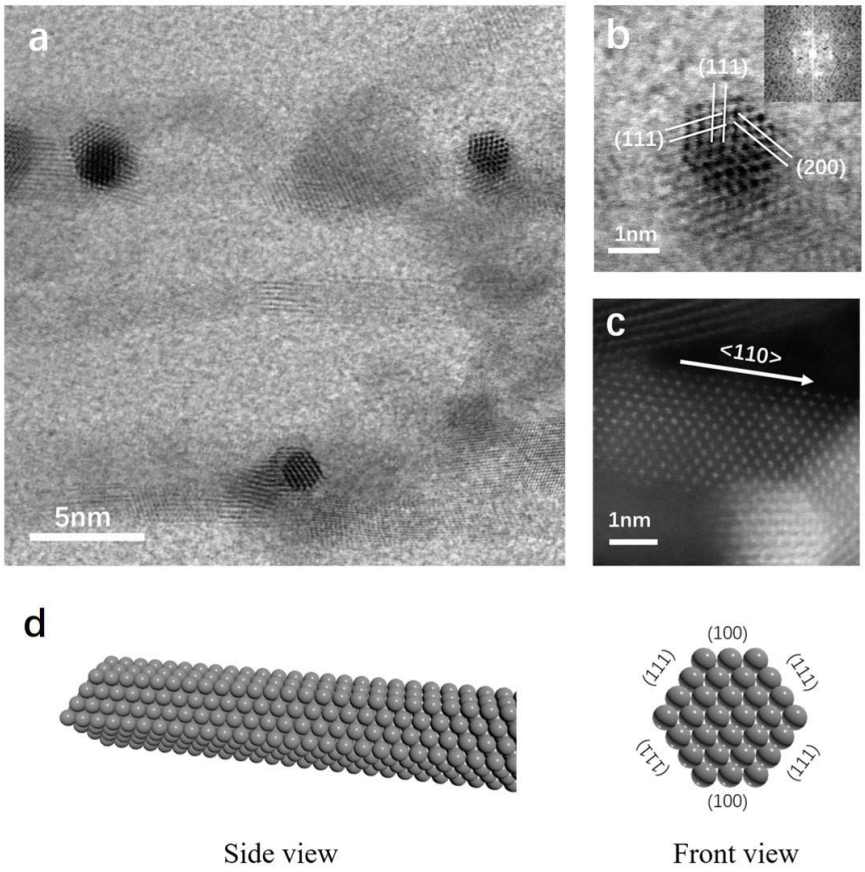

Figure 2-7 Morphology of activated nanowires. (a,b) HRTEM cross-sectional images of activated PtNWs. (c) HRTEM image of PtNWs with a <110> growth axis. (d) Schematic illustration of surface structure of activated PtNWs.

We further carried out DFT calculation with explicit consideration of solvent, pH, and voltage on PtNWs with same surface structure. As shown in Fig. 2-8a, the calculated hydrogen adsorption isotherm at pH=0 exhibited two steps of hydrogen adsorption, corresponding to two hydrogen adsorption peaks in the derived CV curve. The position of H_{upd} and H_{opd} peak showed good consistence with our experimental results. The highest hydrogen coverage was reached at potential of -0.1V with a maximum coverage of 1.51 monolayer (ML). The interfacial atomic structure at -0.1V is illustrated in Fig. 2-8b, which showed not only the Pt(111) and Pt(100) surface were covered with hydrogen, the low-coordinated edge sites were also occupied.

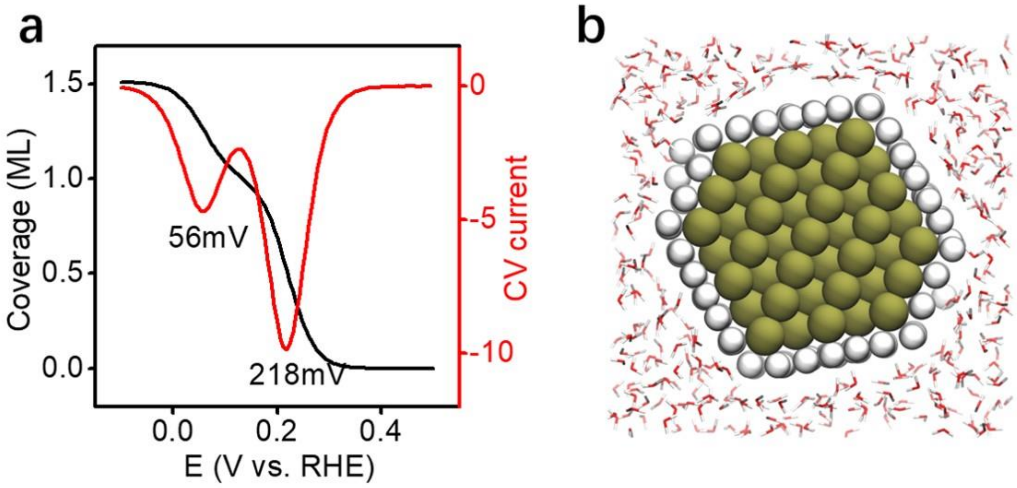

Figure 2-8 Simulation of hydrogen adsorption on PtNWs surface (a) Hydrogen coverage as a function of potential and corresponding CV current as a function of potential. (b) Interfacial atomic structure of nanowire at potential of -0.1V. Dark green atom is Pt, white atom is hydrogen.

To identify the adsorption site of H_{opd}, we further examined the snapshots of interfacial structure at different potential. As shown in Fig. 2-9, the hydrogen first adsorbed on Pt(111) and Pt(100) surface and edge sites were unoccupied till 0.155V. At 0.155V, the overall hydrogen coverage is 0.94ML with Pt(111) and Pt(100) approaching fully covered and then hydrogen started to adsorb on the edge sites. At 0.058V, a potential close to peak potential of H_{opd}, considerable amount of edge sites were occupied. At -0.1V, edge sites were fully covered. To resolve the hydrogen adsorption process on different sites, we counted the number of hydrogen atoms on different sites at each potential in the simulation system. As shown in Fig. 2-10a, hydrogen mainly adsorbed on (111), (100), and edge sites. (111) and (100) surface were firstly covered and the coverage saturated at around 0.1V. Edge sites were occupied at lower potential. To roughly estimate the peak position of hydrogen adsorption on different sites, we carried out nonlinear curve fitting on the adsorption curve and differentiated the fitted results. The result of fitted curves were showed in Fig. 2-10b. The differentiated results showed three hydrogen adsorption peak at 214mV, 210mV, and 76mV, corresponding to hydrogen adsorbed on (100) suface, (111) surface, and edge sites. The addition of three adsorption peaks showed good consistence with the simulated CV curve in Fig. 2-8a. Therefore, the H_{upd} peak at around 0.2V in our theoretial and experimental results originated from hydrogen adsorbed on Pt(111) and Pt(100) surface and the H_{opd} is hydrogen adsorbed on the edge sites. Interestingly, according to previous CV study on Pt(111) single crystal, the hydrogen adsorption curve on Pt(111) is a broad plateau without a significant peak feature[28], however, our result exhibited a peak. Since the Pt(111) surface on the nanowire is a microfacet, it is possible the hydrogen binding energy on such surface is relatively confined, which lead to the formation of a Pt(111)

peak.

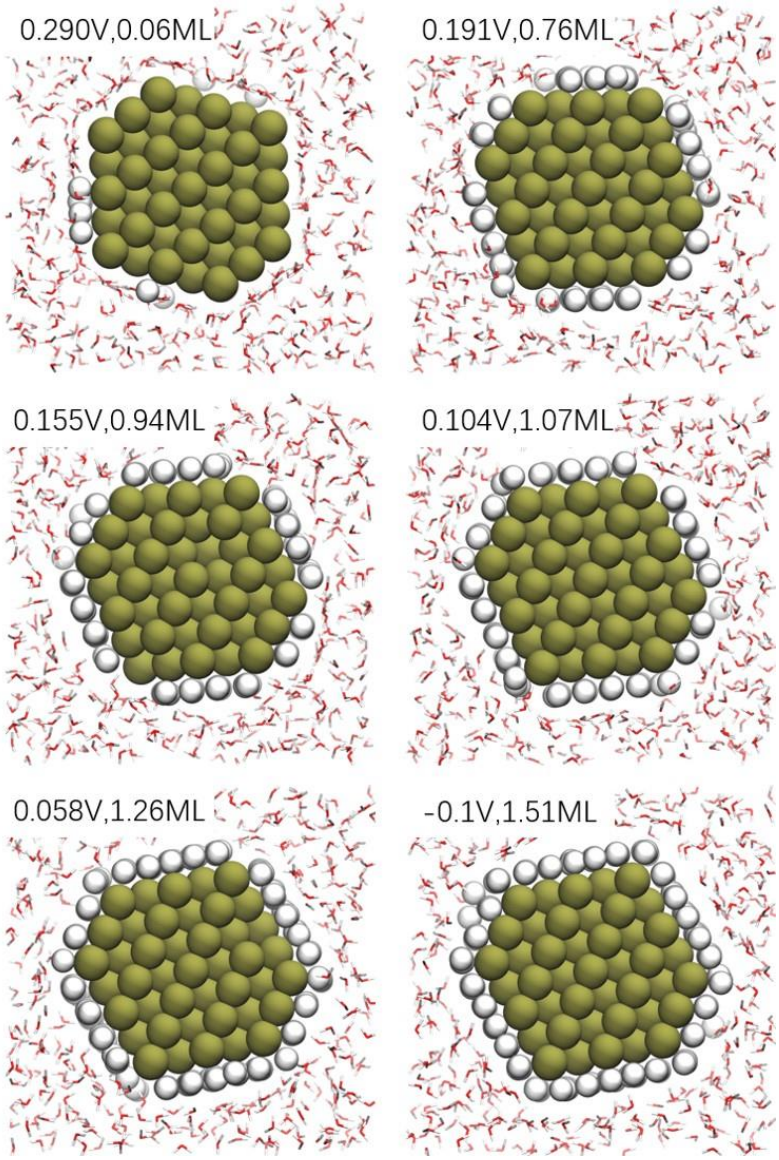

Figure 2-9 Snapshots of interfacial structure at different potentials.

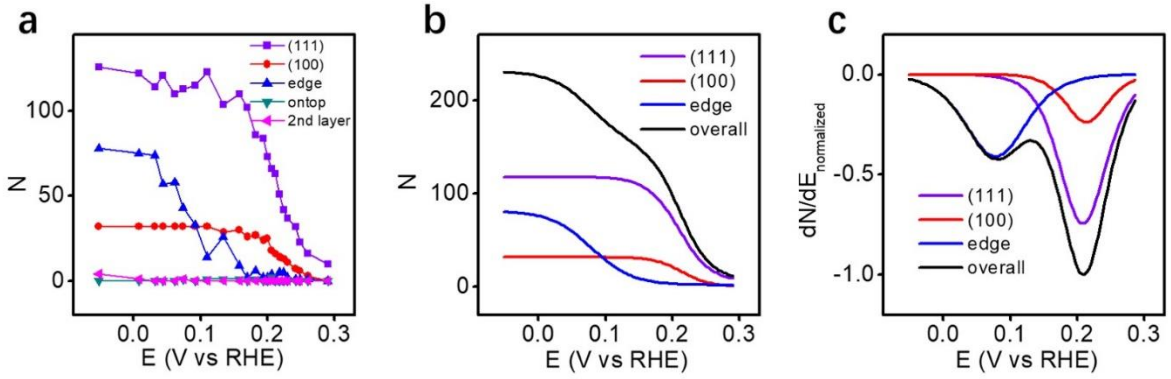

Figure 2-10 (a) Number of hydrogen on different sites as a function of potential. (b) Nonlinear curve fitting of hydrogen number on different sites as a function of potential. The overall curve is the addition of curves of (111), (100), and edge. (c) Derivative of fitted curves from (b). The result is normalized to the peak value at 0.21V in the overall curve.

Hydrogen on edge sites is an ontop hydrogen, which is considered kinetically active for HER. In acidic solution, Volmer step has low energy barrier, the reaction rate is determined by Tafel step or Heyrovsky step. For these two steps to proceed, at transition state, hydrogen that originally stay on hollow sites or bridge sites have to activated to the ontop sites, which then interact with another ontop hydrogen or approaching proton to from H_2[29]. It is suggested the weakly bound ontop hydrogen is kinetically active for HER, while H_{upd} is kinetically inactive. The presence of H_{upd} hydrogen promotes adsorption of ontop hydrogen, which allows the reaction to proceed through a more facile, on-top mechanism[30]. From our simulation results, it is found there was no ontop hydrogen on Pt(100) and Pt(111) surface in the interested potential range. While the hydrogen adsorbed on the edge sites has lower binding energy and it is also on the top sites, which allows the on-top mechanism. It is also proposed that the reaction pathway on stepped Pt(211) proceed with one ontop hydrogen on the edge site reacting with another hydrogen from terrace site[29]. Therefore, we concluded that the H_{opd} that adsorbed on edge site is the reactive intermediate of HER, which governs reaction rate of HER.

2.4 Conclusion

In summary, we fabricated a faradaic transistor using ultrathin PtNWs with well-defined surface structure to monitor hydrogen adsorption behavior on the surface and investigate reaction intermediate of HER. Molecules or atoms that adsorbed on surface can alter surface scattering of conduction electrons, leading to the conductance change. Based on this principle,

a faradaic transistor was designed to measure the conductance change of catalyst in electrochemical environment, which provided information on the electrochemical interface. In our study, a significant conductance increase was observed in hydrogen adsorption region, which indicated adsorption of hydrogen is accompanied with desorption of water. This is important for understanding HER mechanism and kinetics from perspective of water adsorption behaviors. A derivative approach was used to differentiate conductance change, which provided a profile correlated to the CV curve. A new hydrogen adsorption peak near equilibrium potential was resolved for the first time. We assigned this hydrogen adsorption peak as H_{opd} peak. Our simulation study showed this H_{opd} peak originated from hydrogen adsorbed on edge sites. The ontop nature and lower hydrogen binding energy make this edge site hydrogen more active, therefore, we proposed this edge site hydrogen is the reaction intermediate.

2.5 References

1. Skúlason, E.; Jónsson, H., Atomic scale simulations of heterogeneous electrocatalysis: recent advances. *Advances in Physics: X* **2017,** *2* (3), 481-495.

2. Jaramillo, T. F.; Jørgensen, K. P.; Bonde, J.; Nielsen, J. H.; Horch, S.; Chorkendorff, I., Identification of Active Edge Sites for Electrochemical H₂ Evolution from MoS₂ Nanocatalysts. *Science* **2007,** *317* (5834), 100-102.

3. Skúlason, E.; Tripkovic, V.; Björketun, M. E.; Gudmundsdóttir, S.; Karlberg, G.; Rossmeisl, J.; Bligaard, T.; Jónsson, H.; Nørskov, J. K., Modeling the Electrochemical Hydrogen Oxidation and Evolution Reactions on the Basis of Density Functional Theory Calculations. *The Journal of Physical Chemistry C* **2010,** *114* (42), 18182-18197.

4. Nørskov, J. K.; Rossmeisl, J.; Logadottir, A.; Lindqvist, L.; Kitchin, J. R.; Bligaard, T.; Jónsson, H., Origin of the Overpotential for Oxygen Reduction at a Fuel-Cell Cathode. *The Journal of Physical Chemistry B* **2004,** *108* (46), 17886-17892.

5. Liu, X.; Yang, W.; Liu, Z., Recent Progress on Synchrotron-Based In-Situ Soft X-ray Spectroscopy for Energy Materials. *Advanced Materials* **2014,** *26* (46), 7710-7729.

6. Velasco-Velez, J.-J.; Wu, C. H.; Pascal, T. A.; Wan, L. F.; Guo, J.; Prendergast, D.; Salmeron, M., The structure of interfacial water on gold electrodes studied by x-ray absorption spectroscopy. *Science* **2014,** *346* (6211), 831-834.

7. Kunimatsu, K.; Senzaki, T.; Samjeské, G.; Tsushima, M.; Osawa, M., Hydrogen adsorption and hydrogen evolution reaction on a polycrystalline Pt electrode studied by surface-enhanced infrared absorption spectroscopy. *Electrochimica Acta* **2007,** *52* (18), 5715-5724.

8. Zhu, S.; Qin, X.; Yao, Y.; Shao, M., pH-Dependent Hydrogen and Water Binding Energies on Platinum Surfaces as Directly Probed through Surface-Enhanced Infrared Absorption Spectroscopy. *Journal of the American Chemical Society* **2020,** *142* (19), 8748-8754.

9. Dong, J.-C.; Zhang, X.-G.; Briega-Martos, V.; Jin, X.; Yang, J.; Chen, S.; Yang, Z.-L.; Wu, D.-Y.; Feliu, J. M.; Williams, C. T.; Tian, Z.-Q.; Li, J.-F., In situ Raman spectroscopic evidence for oxygen reduction reaction intermediates at platinum single-crystal surfaces. *Nature Energy* **2019,** *4* (1), 60-67.

10. Conway, B. E.; Tilak, B. V., Interfacial processes involving electrocatalytic evolution and oxidation of H2, and the role of chemisorbed H. *Electrochimica Acta* **2002,** *47* (22), 3571-3594.

11. Sondheimer, E. H., The mean free path of electrons in metals. *Advances in Physics* **2001,** *50* (6), 499-537.

12. Wißmann, P., The electrical resistivity of pure and gas covered metal films. In *Surface Physics*, Springer Berlin Heidelberg: Berlin, Heidelberg, 1975; pp 1-96.

13. Fuchs, K., The conductivity of thin metallic films according to the electron theory of metals. *Mathematical Proceedings of the Cambridge Philosophical Society* **1938,** *34* (1), 100-108.

14. Yang, F.; Donavan, K. C.; Kung, S.-C.; Penner, R. M., The Surface Scattering-Based Detection of Hydrogen in Air Using a Platinum Nanowire. *Nano Letters* **2012,** *12* (6), 2924-2930.

15. Fujihara, M.; Kuwana, T., Studies of electrochemical interfaces of thin PT film electrodes by surface conductance. *Electrochimica Acta* **1975,** *20* (8), 565-573.

16. Tucceri, R. I.; Posadas, D., The effect of surface charge on the surface conductance of silver in surface inactive electrolytes. *Journal of Electroanalytical Chemistry and Interfacial Electrochemistry* **1990,** *283* (1), 159-166.

17. Tucceri, R., A review about the surface resistance technique in electrochemistry. *Surface Science Reports* **2004,** *56* (3), 85-157.

18. Ding, M.; He, Q.; Wang, G.; Cheng, H.-C.; Huang, Y.; Duan, X., An on-chip electrical transport spectroscopy approach for in situ monitoring electrochemical interfaces. *Nature Communications* **2015,** *6*, 7867.

19. Li, M.; Zhao, Z.; Cheng, T.; Fortunelli, A.; Chen, C.-Y.; Yu, R.; Zhang, Q.; Gu, L.; Merinov, B. V.; Lin, Z.; Zhu, E.; Yu, T.; Jia, Q.; Guo, J.; Zhang, L.; Goddard, W. A.; Huang, Y.; Duan, X., Ultrafine jagged platinum nanowires enable ultrahigh mass activity for the oxygen reduction reaction. *Science* **2016,** *354* (6318), 1414-1419.

20. ZIman, J. M., The principles of the theory of solids. *Cambridge University Press* **1972**.

21. Dasgupta, S.; Kruk, R.; Ebke, D.; Hütten, A.; Bansal, C.; Hahn, H., Electric field induced reversible tuning of resistance of thin gold films. *Journal of Applied Physics* **2008,** *104* (10), 103707.

22. Sagmeister, M.; Brossmann, U.; Landgraf, S.; Würschum, R., Electrically Tunable Resistance of a Metal. *Physical Review Letters* **2006,** *96* (15), 156601.

23. Zheng, J.; Nash, J.; Xu, B.; Yan, Y., Perspective—Towards Establishing Apparent Hydrogen Binding Energy as the Descriptor for Hydrogen Oxidation/Evolution Reactions. *Journal of The Electrochemical Society* **2018,** *165* (2), H27-H29.

24. Cheng, T.; Wang, L.; Merinov, B. V.; Goddard, W. A., Explanation of Dramatic pH-Dependence of Hydrogen Binding on Noble Metal Electrode: Greatly Weakened Water Adsorption at High pH. *Journal of the American Chemical Society* **2018**.

25. Diaz-Morales, O.; Hersbach, T. J. P.; Badan, C.; Garcia, A. C.; Koper, M. T. M., Hydrogen adsorption on nano-structured platinum electrodes. *Faraday Discussions* **2018,** *210* (0), 301-315.

26. Herring, C., Some Theorems on the Free Energies of Crystal Surfaces. *Physical Review* **1951,** *82* (1), 87-93.

27. Wu, Y.; Cui, Y.; Huynh, L.; Barrelet, C. J.; Bell, D. C.; Lieber, C., Controlled Growth and Structures of Molecular-Scale Silicon Nanowires. *Nano Letters* **2004,** *4*, 433-436.

28. Strmcnik, D.; Tripkovic, D.; van der Vliet, D.; Stamenkovic, V.; Marković, N. M., Adsorption of hydrogen on Pt(111) and Pt(100) surfaces and its role in the HOR. *Electrochemistry Communications* **2008,** *10* (10), 1602-1605.

29. Fang, Y.-H.; Wei, G.-F.; Liu, Z.-P., Catalytic Role of Minority Species and Minority Sites

for Electrochemical Hydrogen Evolution on Metals: Surface Charging, Coverage, and Tafel Kinetics. *The Journal of Physical Chemistry C* **2013,** *117* (15), 7669-7680.

30. Lindgren, P.; Kastlunger, G.; Peterson, A. A., A Challenge to the G ~ 0 Interpretation of Hydrogen Evolution. *ACS Catalysis* **2020,** *10* (1), 121-128.

Chapter 3 Faradaic transistor for directly probing pH-dependent hydrogen coverage on platinum surface

3.1 Introduction

Hydrogen evolution reaction (HER) is an essential reaction for the renewable generation of hydrogen by water electrolysis. Platinum (Pt) has been demonstrated to be the most efficient element for catalyzing HER in acidic solution[1]. In proton exchange membranes (PEMs) water electrolyzer, small amount of Pt is required due to its high activity. However, in the anode side, the oxygen evolution reaction (OER) requires large amount of noble metal based catalysts, such as IrO_2, Ru, due to the high overpotential of OER[2-4]. Substantial efforts have been devoted to reducing the costs of catalysts. Many non-noble metal oxide catalysts have been demonstrated to be highly efficient for OER in alkaline solution[5-7]. Unfortunately, for yet unclear reason, the reaction rate of HER in alkaline solution is two orders of magnitude lower than that in acidic solution. Fundamental understanding of the origin of this pH-dependent HER activity is important for further development of alkaline electrolyzers.

The HER in alkaline solution generally proceeds with an initial Volmer step ($H_2O + e^- + M = M - H + OH^-$), including water dissociation and formation of hydrogen intermediates (H_{ad}), and then generate H_2 by either electrochemical Heyrovsky step ($H_2O + M - H + e^- = M + H_2 + OH^-$) or Tafel recombination step ($2M - H = 2M + H_2$). Subbaraman et al. attributed the slower HER kinetics in alkaline solution to the sluggish water dissociation process in alkaline solution. They found $Ni(OH)_2$ clusters on Pt surface can significantly improve HER activity in alkaline solution and proposed $Ni(OH)_2$ can facilitate the dissociation of water and enhance generation of H_{ad} on the adjacent Pt surface and thus increase HER reaction rate[8].

Sheng et al. observed the peak position of H_{upd} linearly increased with the pH, which is correlated to the pH-dependent HER activity. They suggested the hydrogen binding energy (HBE), determined from peak position of H_{upd}, is the sole reaction descriptor for HER and the slower HER reaction rate in alkaline solution is due to the stronger HBE at high pH. The same group later refined the theory and proposed it is apparent hydrogen binding energy (HBE_{app}) that is pH-dependent and determined by peak position of H_{upd}[9]. In their hypothesis, hydrogen adsorption is accompanied by water desorption process and HBE_{app} that take account of both intrinsic HBE and water adsorption energy should be the real descriptor of HER. They further proposed the stronger HBE_{app} in alkaline solution is due to weakened water adsorption in alkaline solution. Cheng et al. later verified this hypothesis by quantum mechanics molecular dynamics simulation[10]. They found Pt surface tends to repel interfacial water at high pH, which in turn increases the hydrogen binding. In spite of the success of HBE_{app} theory in correlating pH-dependent HER activity to H_{upd} peak position on polycrystalline platinum, it has difficulty to explain the HER activity on Pt(111) surface. The H_{upd} of Pt(111) doesn't have noticeable shift with pH, however, Pt(111) still exhibited significant pH-dependent HER kinetics[11]. The structure of electrical double layer is also considered plays an important role in determining reaction kinetics. Koper et al. found the potential of zero free charge (pzfc) shifted further from hydrogen adsorption region with increasing pH[11]. As a result, in alkaline solution, the interfacial water structure is more rigid due to stronger interfacial electrical field, which requires higher water reorganization energy to transport produced OH^- and thus make the Volmer step slower. Recently, Zhu et al. employed surface-enhanced infrared absorption spectroscopy to monitor the electrochemical interface at HER potential and found the binding

energy of ontop hydrogen (H_{atop}) and water both weakened with increasing pH[12]. Since H_{atop} has positive Gibbs free energy, the weakened binding energy push free energy away from 0eV and thus lowered the HER activity[12]. The weakened water binding is considered to be unfavorable for the charge transfer, which also make reaction kinetics slower.

Although many theoretical and experimental works have been done to understand the origin of pH-dependent HER kinetics, up to now, there is no unified descriptor for the reaction. Since Volmer step is the rate-determining step for HER in alkaline solution, current theories mainly focus on different aspects of this step, including binding of reactant/product, activation energy, and transport of product, to describe the reaction kinetics. H_{ad} is the sole reaction intermediate of HER, that formed in Volmer step. All the reaction descriptors ultimately determine the adsorbed state of H_{ad} in equilibrium condition, which directly correlate to reaction pathway and reaction rate. Therefore, it is of considerable significance to monitor adsorbed state of H_{ad} in electrochemical environment.

Faradaic transistor has been proved to be an effective tool for probing hydrogen adsorption behaviors on Pt surface under operando conditions. Herein, we used faradaic transistor to monitor the hydrogen intermediates of HER in solutions of pH from 0 to 13. The conductance change of PtNWs in H_{upd} and HER region at each pH was measured. A differentiation method was used to resolve the hydrogen adsorption peak. A hydrogen adsorption peak, corresponding to overpotentially deposited hydrogen (H_{opd}), was observed at each pH, which exhibited a significant pH-dependence on its peak intensity. DFT calculation were carried out to simulate hydrogen adsorption on PtNWs at different pH, which showed consistent result with experimental result. It is previously demonstrated this H_{opd} is hydrogen adsorbed on edge sites,

which is kinetically active for HER. Therefore, we proposed this pH-dependent H_{opd} coverage is the origin of pH-dependent HER activity. Further kinetic analysis indicated the reaction mechanism of HER is also determined by H_{opd} coverage. Hydrogen adsorption behavior on $Pt/Ni(OH)_2$ nanowires was also explored and it is found $Ni(OH)_2$ can significantly enhance the formation of H_{opd}, which promoted HER reaction rate in alkaline solution. Therefore, combining experimental results with theoretical verification, we proposed H_{opd} is the unified descriptor for HER.

3.2 Device preparation and electrochemistry testing

PtNWs device and Pt/NiO nanowire device preparation

PtNWs device preparation is the same as the protocol in Chapter 2. Pt/NiO device preparation is the same as PtNWs device preparation, except the acid treatment time is 5 second and device activation is operated in 0.1M potassium hydroxide solution.

On-chip electrochemistry testing

Electrolytes of pH=0, 1, 2 were prepared with perchloric acid of different concentrations. Electrolytes of pH=3, 4, 5, 6 were prepared with 0.1M citric acid/citrate buffer solution. Electrolyte of pH=13 was prepared with potassium hydroxide. Before testing on-chip CV and conductance at different pH, the PtNWs device was activated in 0.1M $HClO_4$ by CV cycling for 150 cycles. The N_2-saturated electrolytes of different pH were pumped into microfluid system for on-chip electrochemical measurement from pH=0 to 13. Pt/NiO nanowire device was only tested in 0.1M KOH electrolyte. Before testing, the device was activated in 0.1M KOH by CV cycling for 30 cycles.

Electrochemistry testing on rotating disk electrode

The electrochemical testing was performed in a three-electrode cell. The working electrode was prepared by coating the Pt/NiO nanowires directly on glassy carbon electrode. A Ag/AgCl electrode was used as reference. A Pt wire was used as counter electrode. The Pt/NiO nanowires were firstly activated in N_2 saturated 0.1M $HClO_4$ solution by CV cycling for 150 cycles at potential between 0.05 to 1.1V vs. RHE. NiO dissolved during activation. Then, CV of PtNWs was measured in N_2-saturated electrolytes of different pH.

3.3 Results and discussion

We firstly examined the hydrogen adsorption behavior on PtNWs at pH=0, 1, and 2. CV of PtNWs measured on rotating disk electrode (RDE) were shown in Fig. 3-1. In H_{upd} region (0.05-0.40V), the CV curves are very similar in terms of shape and current density. However, at potential below 0.05V, the overpotential of HER significantly increase with pH, which indicated a slower kinetic at higher pH. In mechanistic study, the HER kinetic is conventionally correlated to the binding energy of H_{upd}[1, 13-14]. However, recent theoretical study indicated H_{upd} that adsorbed in the hollow sites is kinetically inactive, while the weakly bound, ontop hydrogen is kinetically active for HER[15-16]. Since such weakly bound hydrogen is formed near or below HER onset potential, CV is incapable to decouple its adsorption current with HER current. Therefore, CV approach cannot provide information to explain this pH dependent HER activity.

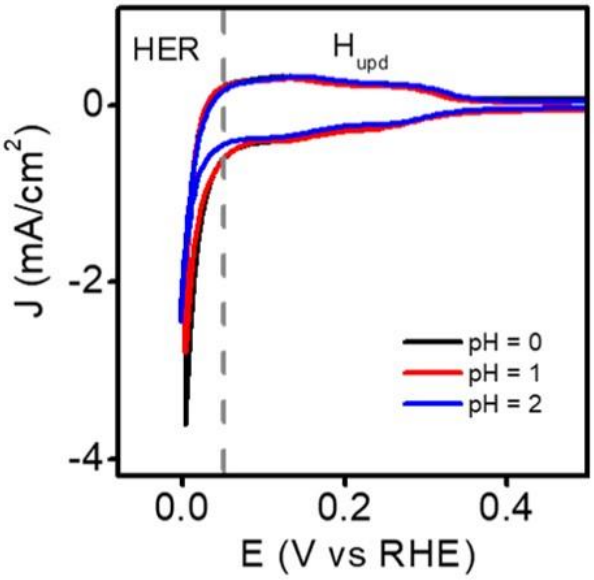

Figure 3-1 CV of PtNWs measured on RDE at pH=0, 1, and 2.

To study hydrogen adsorption behavior in HER region at different pH, faradaic transistor was firstly applied to measure the conductance change of PtNWs in hydrogen adsorption regions at pH=0-2. As shown in Fig. 3-2a, a specific conductance increase was observed in hydrogen adsorption region. The overall conductance changes were 0.055mS, 0.048mS, and 0.046mS for electrolyte of pH=0, 1, and 2, respectively, which indicated decrease of hydrogen coverage with increasing pH. At 0.2-0.4V, conductance changes were similar for three electrolytes. However, at potential below 0.2V, the slopes of conductance change became significantly different. By differentiating the conductance change, as shown in Fig. 3-2b, two hydrogen adsorption peaks were resolved. In our previous simulation study, the peak at around 0.2V is for hydrogen adsorbed on Pt(100) and Pt(111) surface, we assigned this peak as $H_{terrace}$. The peak near 0.05V is for hydrogen adsorbed on edge sites, referring to H_{opd}. It is found the peak intensity of $H_{terrace}$ remained almost unchanged, however, the peak intensity of H_{opd}

significantly decreased with increasing pH. The associated HER reaction rate also showed dramatic decrease with increasing pH. As shown in Fig. 3-2c, at current of 70nA, the overpotential were 27mV, 38mV, and 85mV for electrolytes of pH=0, 1, and 2, respectively, which indicated a decreased kinetics with increasing pH. By plotting the CV current at -0.1V as a function of H_{opd} peak intensity, as shown in Fig. 3-2d, a positive correlation between HER activity and H_{opd} peak intensity was observed. Since H_{opd} is considered as kinetically active reaction intermediate in our previous study, its coverage plays an important role on determining HER reaction rate. Therefore, we proposed the pH-dependent HER activity is due to pH-dependent H_{opd} coverage.

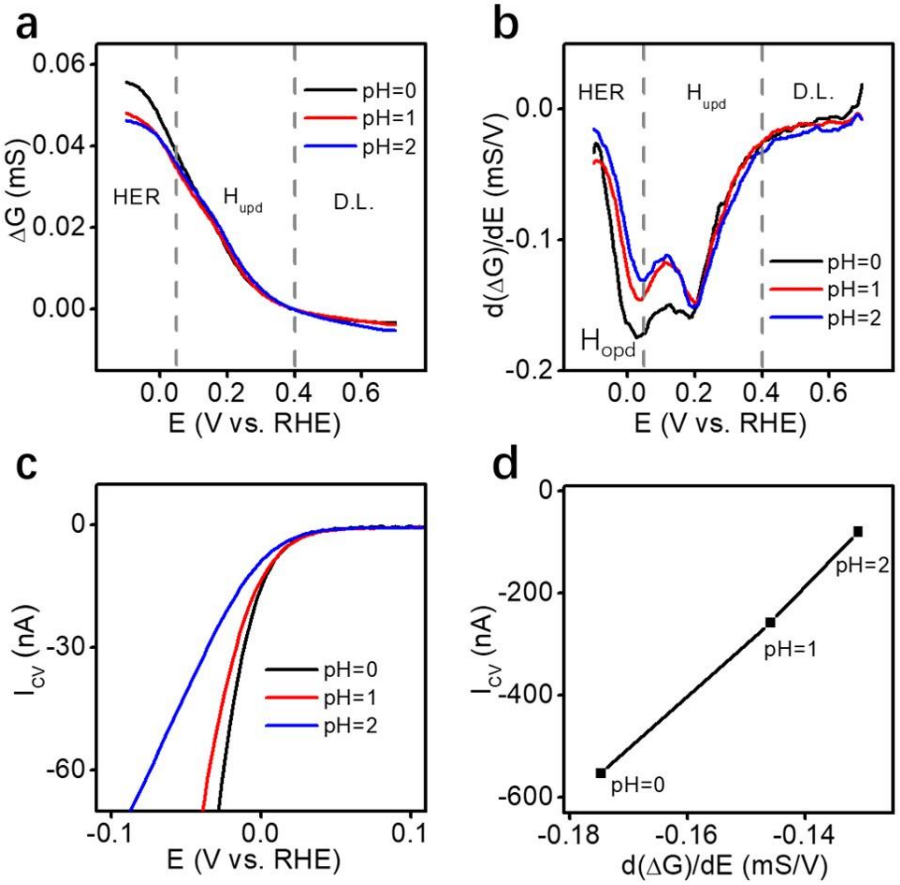

Figure 3-2 (a,b) Conductance change (a) and derivative conductance change (b) of PtNWs in

$HClO_4$ solutions of pH=0-2. (c) On-chip HER polarization curves of PtNWs at pH=0-2. (d) HER current at -0.1V as a function of H_{opd} peak intensity.

To investigate the adsorption behavior of H_{opd} in a more extended pH range, we further examined the H_{opd} peak intensity in citric acid/citrate buffer solutions of pH=3-6. Different with $HClO_4$ electrolyte where ClO_4^- has negligible interaction with surface, these buffer solutions have cations and anions which may interact with Pt surface. The conductance change of PtNWs is shown in Fig. 3-3a, which showed significantly different conductance change at potential lower than 0.2V. The corresponding derivative conductance change, as shown in Fig. 3-3b, also exhibited a $H_{terrace}$ peak and a much smaller H_{opd} peak. The $H_{terrace}$ peak intensity in citric acid/citrate buffer solution is stronger than that in 0.1M $HClO_4$ solution. This is due to adsorption of citric acid and citrate anion on the surface, which provided extra scattering centers and led to a more significant conductance change in hydrogen adsorption and surface species desorption processes. The $H_{terrace}$ peak intensity also showed slight difference in different buffer solutions due to different concentration of citric acid and citric anion. For H_{opd} peak, at pH=3-6, their peak intensities are significantly smaller than that at pH=1. From pH=3 to 6, not only the peak intensity of H_{opd} decreased, the shape of the peak also changed from a clear peak feature to a plateau. Therefore, we conclude that this H_{opd} peak is also diminishing from pH=3 to 6. A positive correlation between HER current and H_{opd} peak intensity is also observed at pH=3-6, as shown in Fig. 3-3c.

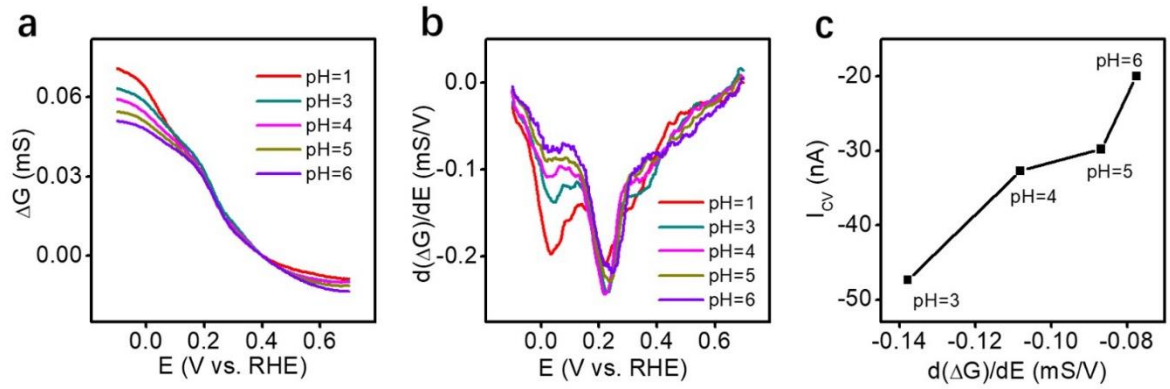

Figure 3-3 (a,b) Conductance change (a) and derivative conductance change (b) of PtNWs in electrolytes of pH=1, 3-6. (c) HER current at -0.1V as a function of H_{opd} peak intensity at pH=3-6.

To compare the derivative conductance change result at different pH, especially for electrolytes which have different ions, we further normalized each derivative conductance change curve by setting $H_{terrace}$ peak value to -1. Because $H_{terrace}$ adsorption peak is a dominant peak and Pt(100) and Pt(111) are the dominant facets. We assumed the ratio of different facets don't change after CV profile is stable. Then, the normalized derivative conductance change can be used to evaluate the proportion of H_{opd} on PtNWs surface. As shown in Fig. 3-4a, after normalization, normalized peak intensity of H_{opd} decreased from pH=0 to 6. The normalized H_{opd} peak intensity as a function of pH showed that the maximum change of peak intensity happened between pH=2 and 3 and the peak intensity tended to be stable from pH=4 to 6 (see Fig.3-4b).

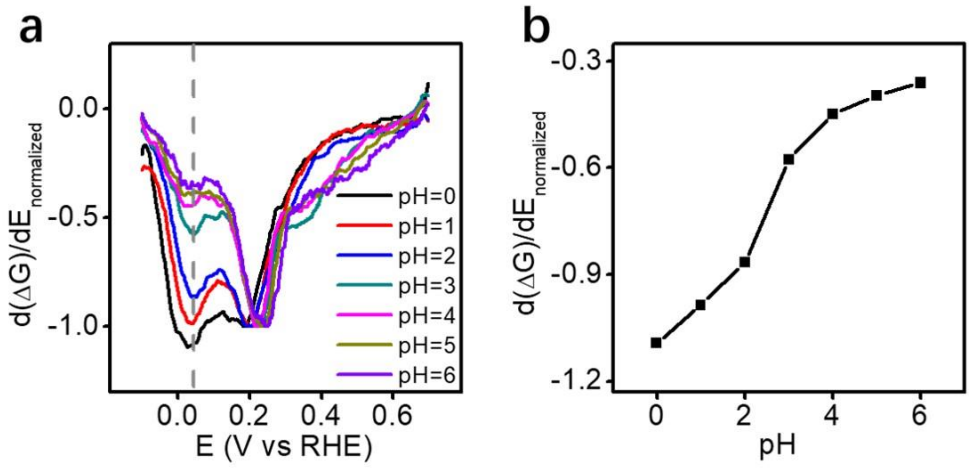

Figure 3-4 (a) Normalized derivative conductance change at pH=0-6. (b) Normalized peak intensity of H_{opd} as a function of pH.

We also carried out DFT calculation to simulate hydrogen adsorption behavior at different pH. The hydrogen coverage as a function of potential was estimated. As shown in Fig. 3-5a, two hydrogen adsorption steps were also observed at all pH. Different hydrogen adsorption behaviors were observed at potential lower than 0.17V. With increasing the pH, the maximum hydrogen coverage decreased. As shown in Fig. 3-5b, from pH=0 to 4, maximum hydrogen coverage linearly decreased from 1.5ML to 1.25ML. The coverage tended to be stable from pH=4 to 6. Hydrogen adsorption current at different potential is also derived, which exhibited two adsorption peaks: $H_{terrace}$ and H_{opd} peak. (see Fig. 3-5c). The H_{opd} peak exhibited a significant pH dependence. The H_{opd} peak intensity as a function of pH, as shown in Fig. 3-5d, showed a linear decrease of peak intensity from pH=0 to 4 and then a slight change from pH=4 to 6. The simulation result showed good consistence with our experimental result. Therefore, combining experimental and theoretical results, we concluded that HER reaction rate is governed by H_{opd} coverage and pH-dependent H_{opd} coverage is the origin of pH-dependent

HER reaction rate.

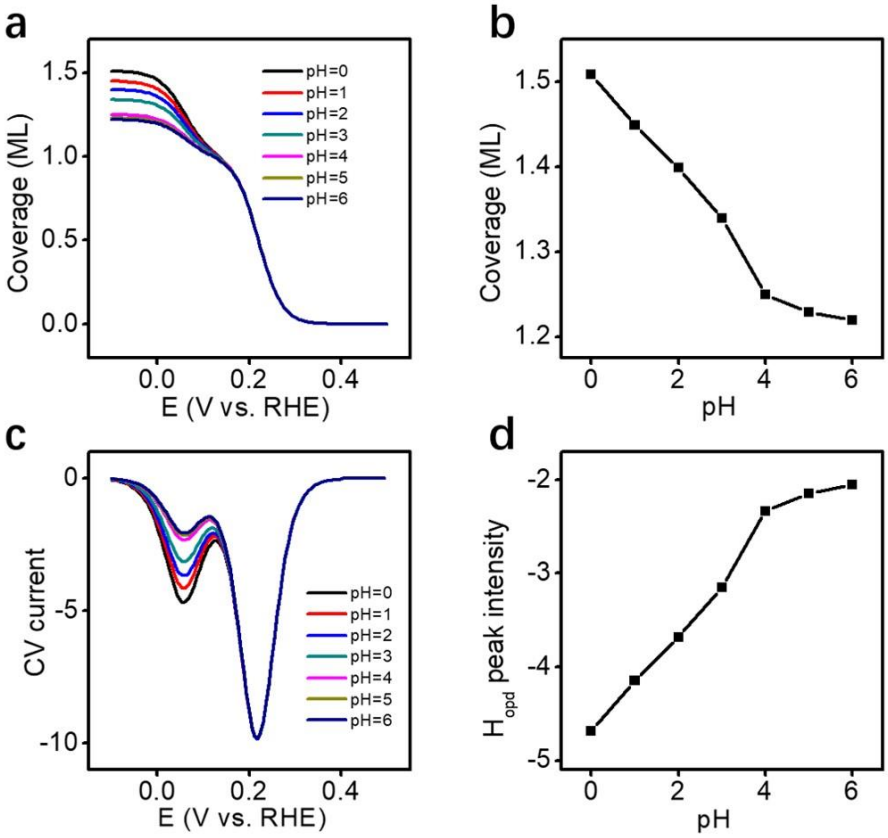

Figure 3-5 (a) Estimated hydrogen coverage as a function of potential at pH=0-6. (b) Maximum hydrogen coverage as a function of pH. (c) Derived hydrogen adsorption current as a function of potential at pH=0-6. (d) Estimated H_{opd} peak intensity as a function of pH.

It is generally accepted that HER reaction rate is determined by different elementary steps in acidic and alkaline conditions. To further explore the relationship between pH dependent H_{opd} peak intensity and HER reaction mechanism, we analyzed the Tafel slope at different pH. The reaction mechanism of HER can be derived from the relationship between driving force (overpotential) and reaction rate (current) in a Tafel plot. As shown in Fig. 3-6a, in the Tafel plot, a linear region was observed near 0V for all pH. In these regions, the reaction current is

mainly controlled by its kinetic. The Tafel slope in these regions were derived and it showed that the Tafel slope increase from about 35mV dec^{-1} to about 100mV dec^{-1} from pH=0 to 6 (see Fig. 3-6b). A maximum increase of Tafel slope were observed between pH=2 and 3 from 49mV dec^{-1} to 79mV dec^{-1}, which may indicate a transition of reaction mechanism from pH=2 to 3. The Tafel plot determined from simulation result also exhibited a similar trend (see Fig. 3-6c,d). Previous experimental results showed the Tafel slope is 30mV dec^{-1} in acid solutions and 120mV dec^{-1} in alkaline solutions[17-18]. Kinetic analysis has assigned experimentally observed Tafel slope to specific rate determining steps[19]. Specifically, when Tafel slope is 30mV dec^{-1}, the rate determining step is Tafel step, as for 120mV dec^{-1}, the rate determining step is Volmer step. In our results, we observed there is a gradual change of Tafel slope from pH=0 to 6. It is suggested the activation energy of each elementary step is sensitive to the local binding environment, including hydrogen coverage and adsorption sites[16, 20-21]. Recent theoretical study showed, to achieve a Tafel slope of ~30 mV/dec, HER has to proceed with a top-top mechanism, wherein two weakly bound hydrogen at top sites recombined to form H_2[15]. At pH=1, the high coverage of ontop hydrogen at edge sites (H_{opd}) will allow the reaction to happen with a more favorable on-top mechanism. Therefore, the reaction rate is controlled by Tafel step. At pH=6, where H_{opd} coverage is significantly smaller, the reaction rate is limited by formation of H_{opd}, so rate-determining step shift to Volmer step. The relationship between Tafel slope and H_{opd} peak intensity is demonstrated in Fig. 3-7, which showed strong correlation between H_{opd} peak intensity and the Tafel slope. Therefore, we concluded that HER reaction mechanism is also determined by H_{opd} coverage.

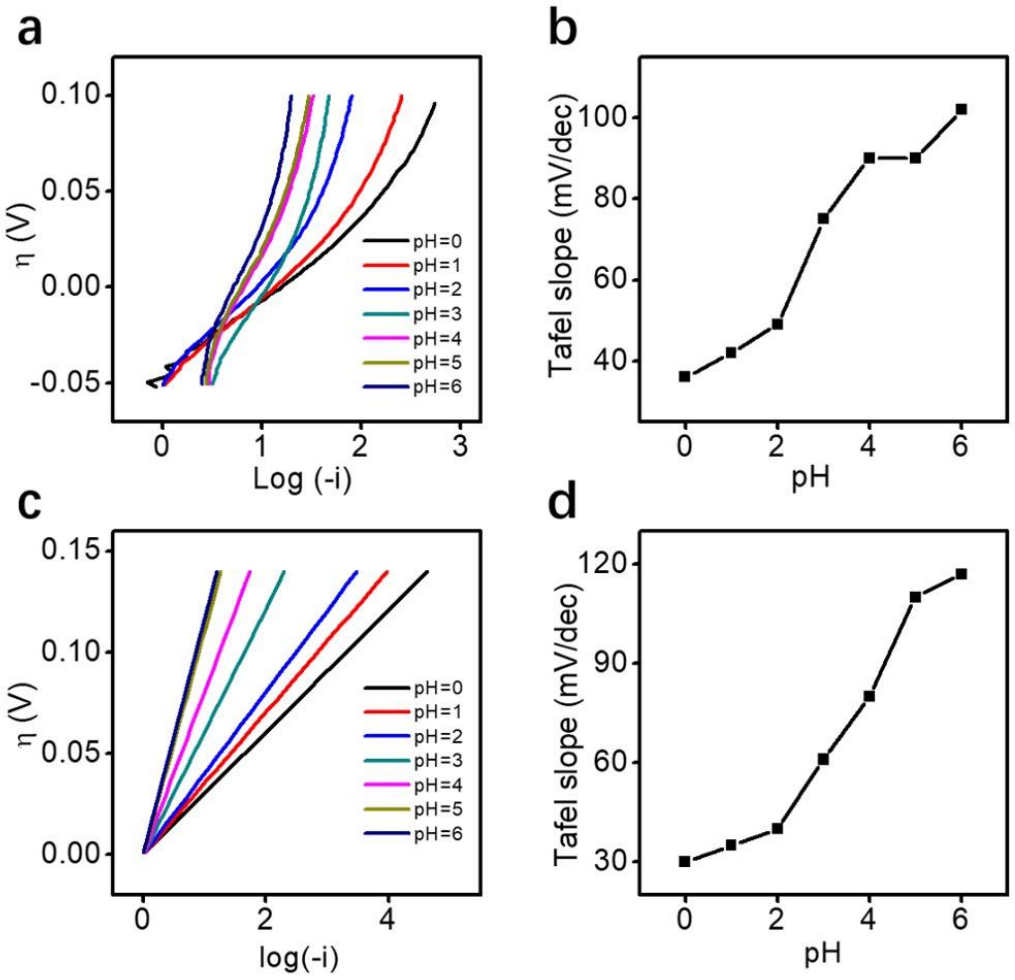

Figure 3-6 (a) Tafel plot at different pH based on on-chip measured HER polarization curves. (b) Tafel slope at different pH (derived from experimental Tafel plot). (c) Tafel plot based on simulated HER polarization curves. (d) Tafel slope at different pH (derived from theoretical Tafel plot)

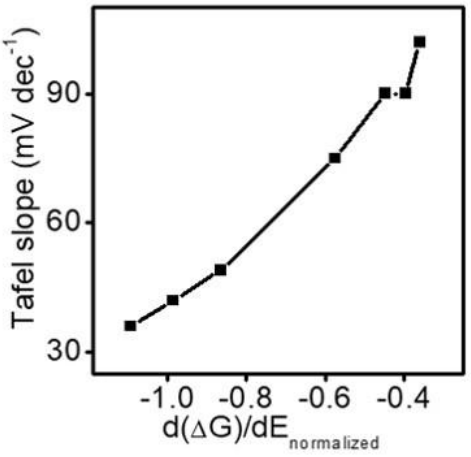

Figure 3-7 Tafel slope as a function of H_{opd} peak intensity (based on experimental results).

With the well establishment of relationship between HER kinetics and H_{opd} coverage in acid media, we further explored the origin of the sluggish kinetics of HER in alkaline solution. The conductance change of PtNWs in hydrogen adsorption region was recorded in alkaline solution, as shown in Fig. 3-8a, a significant conductance increase is observed in H_{upd} region, which followed by a slight conductance increase at potential lower than 0.1V. By differentiating the conductance change, a small H_{opd} peak is also observed. The H_{opd} peak intensity in alkaline solution is much smaller than that at pH=1(see Fig. 3-8b), which is considered as the reason for the sluggish HER kinetic in alkaline solution. Since H_{opd} is considered as kinetically active reaction intermediate, the insufficient H_{opd} coverage impedes the further Tafel step and Heyrovsky step, leading to a lower reaction rate. The molecular-level origin of the low H_{opd} coverage is likely because of the more difficult water dissociation process in alkaline solution. To verify this hypothesis, we further examined the hydrogen adsorption process on Pt surface decorated with $Ni(OH)_2$.

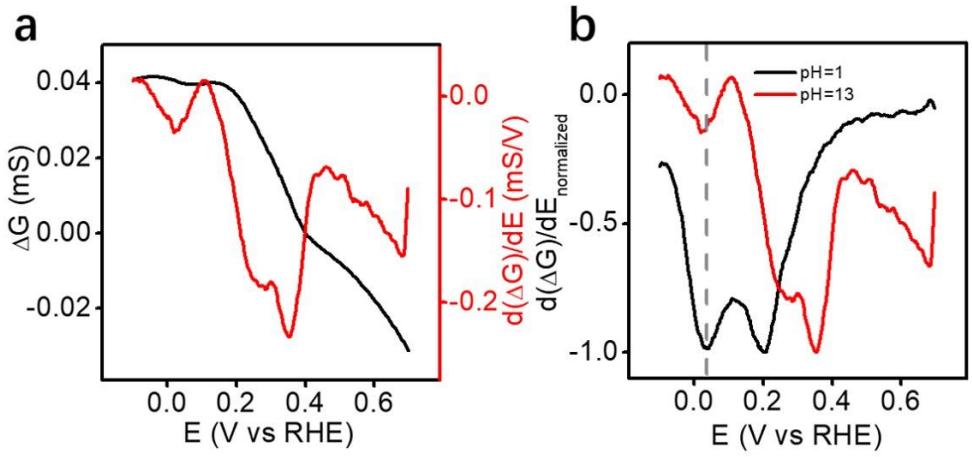

Figure 3-8 (a) Conductance change and corresponding derivative conductance change of PtNWs at potential of (-0.1-0.7V) in 0.1M KOH solution. (b) Comparison of normalized derivation conductance change at pH=1 and 13.

It have been suggested that $Ni(OH)_2$ can greatly boost HER reaction rate on Pt surface in alkaline solution[8, 22]. A bifunctional mechanism was proposed wherein $Ni(OH)_2$ can promote water dissociation process and the production of hydrogen intermediate on the adjacent Pt surface. A direct way to verify this hypothesis is detecting the hydrogen coverage on the surface. Therefore, we examined the conductance change of $Pt/Ni(OH)_2$ in hydrogen adsorption region in alkaline solution and compared it with the results on Pt surface. As shown in Fig. 3-9a, on $Pt/Ni(OH)_2$ surface, a significant conductance increase was observe at potential below 0.1V, while just a slight conductance increase was observe on Pt surface below 0.1V. Since $Ni(OH)_2$ contributed a constant scattering effect on the surface, the conductance change is solely due to interfacial adsorption/desorption process. To compare the derivative conductance change from two different device, a new normalization method was applied. We firstly aligned the $H_{terrace}$ peak to the same height and then normalized the peak intensity to -1. The result is showed in

Fig. 3-9b. A H_{opd} peak was also resolved on Pt/Ni(OH)$_2$ surface, which has much higher peak intensity than that on PtNWs surface. Therefore, we provided a direct evidence that Ni(OH)$_2$ can promote adsorption of hydrogen intermediate, which greatly improved HER reaction rate.

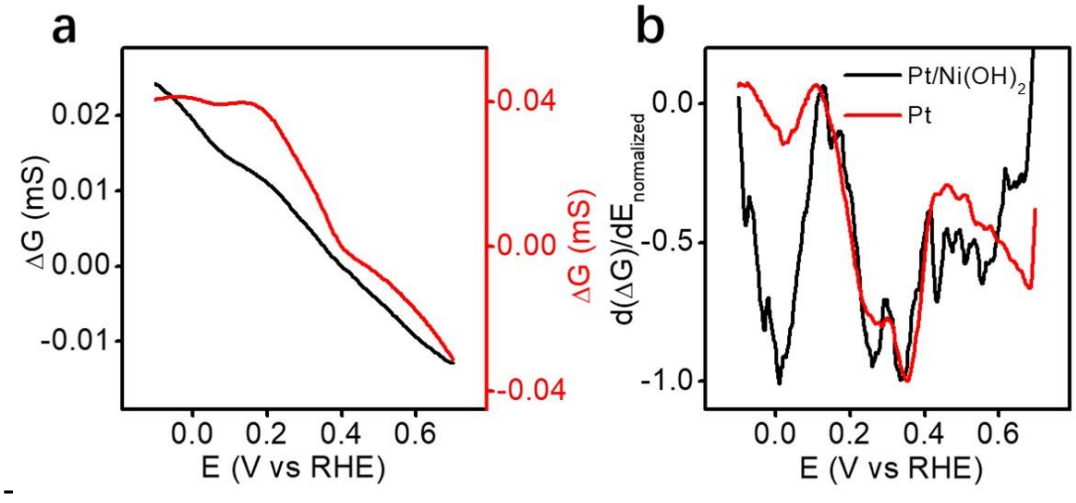

Figure 3-9 (a) Conductance change of Pt/Ni(OH)$_2$ nanowire (black curve) and PtNWs (red curve) in 0.1M KOH solutions. (b) Normalized derivative conductance change of Pt/Ni(OH)$_2$ nanowire and PtNWs in 0.1M KOH solutions.

3.4 Conclusion

In summary, Faradaic transistor is applied to examine the hydrogen adsorption behavior on PtNWs surface at different pH and on Pt/Ni(OH)$_2$ surface in alkaline solution. By measuring the conductance change of nanowires and using a differentiation method, a H_{opd} adsorption peak was observed in electrolytes of different pH. It is found the H_{opd} peak intensity decreased with increasing pH, which is correlated to the pH-dependent HER activity. Further Tafel analysis revealed the HER reaction mechanism is also determined by H_{opd} coverage. DFT calculation exhibited consistent results. Combining theoretical and experimental results, we proposed that coverage of H_{opd} is a unified descriptor for HER and we concluded that the

sluggish reaction rate in alkaline solution is due to insufficient H_{opd} coverage. A molecular-level understanding of the catalytic role of $Ni(OH)_2$ is also provided. The greatly increased H_{opd} coverage on $Pt/Ni(OH)_2$ surface lies at the origin of improved HER activity on $Pt/Ni(OH)_2$ surface.

3.5 References

1. Skúlason, E.; Tripkovic, V.; Björketun, M. E.; Gudmundsdóttir, S.; Karlberg, G.; Rossmeisl, J.; Bligaard, T.; Jónsson, H.; Nørskov, J. K., Modeling the Electrochemical Hydrogen Oxidation and Evolution Reactions on the Basis of Density Functional Theory Calculations. *The Journal of Physical Chemistry C* **2010,** *114* (42), 18182-18197.

2. Durst, J.; Siebel, A.; Simon, C.; Hasché, F.; Herranz, J.; Gasteiger, H. A., New insights into the electrochemical hydrogen oxidation and evolution reaction mechanism. *Energy & Environmental Science* **2014,** *7* (7), 2255-2260.

3. Seh, Z. W.; Kibsgaard, J.; Dickens, C. F.; Chorkendorff, I.; Nørskov, J. K.; Jaramillo, T. F., Combining theory and experiment in electrocatalysis: Insights into materials design. *Science* **2017,** *355* (6321), eaad4998.

4. Reier, T.; Oezaslan, M.; Strasser, P., Electrocatalytic Oxygen Evolution Reaction (OER) on Ru, Ir, and Pt Catalysts: A Comparative Study of Nanoparticles and Bulk Materials. *ACS Catalysis* **2012,** *2* (8), 1765-1772.

5. Hunter, B. M.; Blakemore, J. D.; Deimund, M.; Gray, H. B.; Winkler, J. R.; Müller, A. M., Highly Active Mixed-Metal Nanosheet Water Oxidation Catalysts Made by Pulsed-Laser Ablation in Liquids. *Journal of the American Chemical Society* **2014,** *136* (38), 13118-13121.

6. Zhang, B.; Zheng, X.; Voznyy, O.; Comin, R.; Bajdich, M.; García-Melchor, M.; Han, L.;

Xu, J.; Liu, M.; Zheng, L.; García de Arquer, F. P.; Dinh, C. T.; Fan, F.; Yuan, M.; Yassitepe, E.; Chen, N.; Regier, T.; Liu, P.; Li, Y.; De Luna, P.; Janmohamed, A.; Xin, H. L.; Yang, H.; Vojvodic, A.; Sargent, E. H., Homogeneously dispersed multimetal oxygen-evolving catalysts. *Science* **2016,** *352* (6283), 333-337.

7. McCrory, C. C. L.; Jung, S.; Peters, J. C.; Jaramillo, T. F., Benchmarking Heterogeneous Electrocatalysts for the Oxygen Evolution Reaction. *Journal of the American Chemical Society* **2013,** *135* (45), 16977-16987.

8. Subbaraman, R.; Tripkovic, D.; Strmcnik, D.; Chang, K.-C.; Uchimura, M.; Paulikas, A. P.; Stamenkovic, V.; Markovic, N. M., Enhancing Hydrogen Evolution Activity in Water Splitting by Tailoring Li^+-$Ni(OH)_2$-Pt Interfaces. *Science* **2011,** *334* (6060), 1256-1260.

9. Zheng, J.; Nash, J.; Xu, B.; Yan, Y., Perspective—Towards Establishing Apparent Hydrogen Binding Energy as the Descriptor for Hydrogen Oxidation/Evolution Reactions. *Journal of The Electrochemical Society* **2018,** *165* (2), H27-H29.

10. Cheng, T.; Wang, L.; Merinov, B. V.; Goddard, W. A., Explanation of Dramatic pH-Dependence of Hydrogen Binding on Noble Metal Electrode: Greatly Weakened Water Adsorption at High pH. *Journal of the American Chemical Society* **2018**.

11. Ledezma-Yanez, I.; Wallace, W. D. Z.; Sebastián-Pascual, P.; Climent, V.; Feliu, J. M.; Koper, M. T. M., Interfacial water reorganization as a pH-dependent descriptor of the hydrogen evolution rate on platinum electrodes. *Nature Energy* **2017,** *2*, 17031.

12. Zhu, S.; Qin, X.; Yao, Y.; Shao, M., pH-Dependent Hydrogen and Water Binding Energies on Platinum Surfaces as Directly Probed through Surface-Enhanced Infrared Absorption Spectroscopy. *Journal of the American Chemical Society* **2020,** *142* (19), 8748-8754.

13. Sheng, W.; Zhuang, Z.; Gao, M.; Zheng, J.; Chen, J. G.; Yan, Y., Correlating hydrogen oxidation and evolution activity on platinum at different pH with measured hydrogen binding energy. *Nature Communications* **2015,** *6*, 5848.

14. Zheng, J.; Sheng, W.; Zhuang, Z.; Xu, B.; Yan, Y., Universal dependence of hydrogen oxidation and evolution reaction activity of platinum-group metals on pH and hydrogen binding energy. *Science Advances* **2016,** *2* (3).

15. Lindgren, P.; Kastlunger, G.; Peterson, A. A., A Challenge to the G ~ 0 Interpretation of Hydrogen Evolution. *ACS Catalysis* **2020,** *10* (1), 121-128.

16. Fang, Y.-H.; Wei, G.-F.; Liu, Z.-P., Catalytic Role of Minority Species and Minority Sites for Electrochemical Hydrogen Evolution on Metals: Surface Charging, Coverage, and Tafel Kinetics. *The Journal of Physical Chemistry C* **2013,** *117* (15), 7669-7680.

17. Seto, K.; Iannelli, A.; Love, B.; Lipkowski, J., The influence of surface crystallography on the rate of hydrogen evolution at Pt electrodes. *Journal of Electroanalytical Chemistry and Interfacial Electrochemistry* **1987,** *226* (1), 351-360.

18. Zheng, J.; Yan, Y.; Xu, B., Correcting the Hydrogen Diffusion Limitation in Rotating Disk Electrode Measurements of Hydrogen Evolution Reaction Kinetics. *Journal of The Electrochemical Society* **2015,** *162* (14), F1470-F1481.

19. Shinagawa, T.; Garcia-Esparza, A. T.; Takanabe, K., Insight on Tafel slopes from a microkinetic analysis of aqueous electrocatalysis for energy conversion. *Scientific Reports* **2015,** *5* (1), 13801.

20. Tan, T. L.; Wang, L.-L.; Johnson, D. D.; Bai, K., Hydrogen Deposition on Pt(111) during Electrochemical Hydrogen Evolution from a First-Principles Multiadsorption-Site Study. *The*

Journal of Physical Chemistry C **2013,** *117* (44), 22696-22704.

21. Yang, F.; Zhang, Q.; Liu, Y.; Chen, S., A Theoretical Consideration on the Surface Structure and Nanoparticle Size Effects of Pt in Hydrogen Electrocatalysis. *The Journal of Physical Chemistry C* **2011,** *115* (39), 19311-19319.

22. Subbaraman, R.; Tripkovic, D.; Chang, K.-C.; Strmcnik, D.; Paulikas, A. P.; Hirunsit, P.; Chan, M.; Greeley, J.; Stamenkovic, V.; Markovic, N. M., Trends in activity for the water electrolyser reactions on 3d M(Ni,Co,Fe,Mn) hydr(oxy)oxide catalysts. *Nature Materials* **2012,** *11*, 550.

Chapter 4 Conclusion

In conclusion, we fabricated a faradaic transistor, which enable us to identify reaction intermediate of specific reaction and can provide information about coverage of surface species in an electrochemical environment. These advantages allow us to investigate the relationship between surface adsorbed state of reaction intermediates and reaction kinetics.

In our first work, we used ultrathin PtNWs with well-defined surface structure to fabricate a faradaic transistor. By measuring the conductance change of the nanowires, the hydrogen adsorption process on PtNWs was resolved. The specific conductance increase in hydrogen adsorption region gave direct evidence that hydrogen adsorption is accompanied with water desorption process, which provided a new insight into understanding HER kinetics from a perspective of water adsorption behavior. A differentiation method was adopted to analyze the conductance change. Hydrogen adsorption peak was successfully resolved by this method. A H_{opd} adsorption peak was resolved for the first time. Additional simulation results determined that H_{opd} is hydrogen adsorbed on the edge sites. Due to the lower binding energy and on-top nature of H_{opd}, we proposed H_{opd} is reactive intermediate of HER.

In our second work, we used this faradaic transistor to investigate pH-dependent HER activity. The conductance change of PtNWs in hydrogen adsorption region at different pH was measured. By using the same differentiation approach, a H_{opd} peak was resolved at each pH, which exhibited a significant pH-dependence. Further simulation results provided consistent results. We concluded HER reaction rate is controlled by H_{opd} coverage and the sluggish HER kinetics in alkaline solution is due to low H_{opd} coverage. Further Tafel analysis demonstrated HER reaction mechanism strongly correlated to H_{opd} coverage. We proposed HER reaction

mechanism is also determined by H_{opd} coverage. Therefore, H_{opd} coverage is considered as a unified descriptor for HER. Catalytic role of $Ni(OH)_2$ for HER in alkaline solution is also investigated. It is found $Ni(OH)_2$ can greatly improve H_{opd} coverage on Pt surface, which is considered as the origin of improved HER activity in alkaline solution.